Mathematical Biosciences 324 (2020) 108326

Contents lists available at ScienceDirect

Mathematical Biosciences

journal homepage: www.elsevier.com/locate/mbs

Original research article

Modelling triatomine bug population and *Trypanosoma rangeli* transmission dynamics: Co-feeding, pathogenic effect and linkage with chagas disease

Xiaotian Wu[a,*], Daozhou Gao[b], Zilong Song[c], Jianhong Wu[d]

[a] College of Arts and Sciences, Shanghai Maritime University, Shanghai, PR China
[b] Department of Mathematics, Shanghai Normal University, Shanghai, PR China
[c] Department of Mathematics, University of California– Riverside, Riverside, CA, United States
[d] Laboratory for Industrial and Applied Mathematics, Department of Mathematics and Statistics, York University, Toronto, Canada

ARTICLE INFO

Keywords:
Trypanosoma rangeli
Chagas disease
Mathematical modelling
Co-feeding transmission
Pathogenic effect
Periodic oscillations

ABSTRACT

Trypanosoma rangeli (*T. rangeli*), a parasite, is not pathogenic to human but pathogenic to some vector species to induce the behavior changes of infected vectors and subsequently impact the transmission dynamics of other diseases such as Chagas disease which shares the same vector species. Here we develop a mathematical model and conduct qualitative analysis for the transmission dynamics of *T. rangeli*. We incorporate both systemic and co-feeding transmission routes, and account for the pathogenic effect using infection-induced fecundity and fertility change of the triatomine bugs. We derive two thresholds $\mathcal{R}_v$ (the triatomine bug basic reproduction number) and $\mathcal{R}_0$ (the *T. rangeli* basic reproduction number) to delineate the dynamical behaviors of the ecological and epidemiological systems. We show that when $\mathcal{R}_v > 1$ and $\mathcal{R}_0 > 1$, a unique parasite positive equilibrium E^* appears. We find that E^* can be unstable and periodic oscillations can be observed where the pathogenic effect plays a significant role. Implications of the qualitative analysis and numerical simulations suggest the need of an integrative vector-borne disease prevention and control strategy when multiple vector-borne diseases are transmitted by the same set of vector species.

1. Introduction

Chagas disease or American trypanosomiasis is a vector-borne disease caused by the causative agent of the protozoan parasite *Trypanosoma cruzi* (*T. cruzi*). Chagas disease, recognized as one of the most neglected diseases, can cause severe life-threatening cardiac and gastrointestinal illness if a patient does not get treatment timely [1]. An estimate of approximately 5 to 10 million people is infected with *T. cruzi* around the world and more than 25 million people are at risk of acquiring the disease, mainly in Latin America [2,3]. Chagas disease has already a wide geographical distribution and is spreading into other continents. It has been recently detected in the United States, Canada and many European and some Western Pacific countries because of enhanced travel means and global population movement [4–6].

T. cruzi is primarily transmitted by a broad range of blood-sucking triatomine species. Infected bugs feed on blood and then deposit their faeces with parasites inside on the hosts' skin. These parasites enter the body through the bite wound site induced by hosts' scratching or rubbing, or other means like urine, and eventually penetrate the hosts' booldstream [1,7,8]. Triatomine bugs (*Hemiptera: Reduviidae*), playing a major role in spreading Chagas disease, have a relatively short and variable lifespan varying from 4 to 14 months which largely rely upon the species and the surrounding environmental conditions. These bugs are not only hematophagous in that bloodmeals are necessary food for their survival and inter-stage development, but also are fast feeders which could release the faeces within the first minutes in a blood meal [9,10]. Moreover, once these homometabolic insects ingest with the parasites of Chagas disease, these parasites develop and multiply quickly inside and make the insects reaching infectious stage quickly within life-span of these insect vectors [9,11].

T. cruzi has a rich range of host species including wildlife (e.g., raccoon and opossum) and domestic animals (e.g., human, dog and cat) and so on, and it is reported that over 100 mammalian species are the natural hosts and susceptible to the infection [12,13]. However, the ability to transmit the Chagas disease parasites varies with host species because of their functional differences. Generally, mammalian animals such as humans, dogs and cats are recognized as the competent hosts, while avian animals such as birds and chickens are recognized as dead-end hosts which just serve as triatomine food sources [13,14].

Many mathematical models have been developed to understand the

* Corresponding author.
E-mail address: wxt1109@163.com (X. Wu).

https://doi.org/10.1016/j.mbs.2020.108326
Received 7 November 2019; Received in revised form 18 February 2020; Accepted 18 February 2020
Available online 22 February 2020

transmission dynamics and evaluate control interventions of Chagas disease. Many of these modelling studies have focused on the interaction between humans and vectors by taking into account different transmission routes (blood transfusion, congenital and vector biting) and different stages of infection in human population (acute and chronic) [3,15,16]. Some of these studies have explored the temporal and/or spatial variations in abundance or persistence-extinction of triatomine population [17–23]. Several studies have also considered the dynamics of disease transmission in the host community composition and hosts' movement behaviors [8,12,24–26]. A few studies have addressed the issues of design and optimization of control strategies and the relevant cost-benefits of managing these interventions [27–31]. Nevertheless, these studies have been limited to the transmission of Chagas disease related to the parasites *T. cruzi*.

Highly relevant to the Chagas disease transmission dynamics is the population dynamics of triatomine species *Rhodnius prolixus* (*R. prolixus*) and the transmission of *Trypanosoma rangeli* (*T. rangeli*) for several reasons described below. Although little attention has been paid on modelling its transmission dynamics, *T. rangeli* as a Trypanosomatidae also infects mammals including humans through the same triatomines [10,32] in various Chagas disease endemic areas [33,34] and spreads in a wide geographical range worldwide through the interaction between hosts and triatomine vectors including in particular *R. prolixus*. Although *T. rangeli* is not pathogenic to human, understanding the transmission dynamics of *T. rangeli* is important for a number of reasons relevant to the interventions of Chagas disease. First of all, *T. rangeli* shares at least 60% antigens with *T. cruzi*, leading to crossed serological reactions and false positive diagnosis of Chagas disease [10,32]. Secondly, *T. rangeli* and *T. cruzi* have large overlaps of geographic distribution, and share many of the vertebrate hosts and triatomine bugs. Behaviors of these vertebrate hosts and triatomine bugs influenced by their infection of *T. rangeli* can impact the effectiveness of the transmission of *T. cruzi*. In addition, *T. rangeli* is currently being experimented with as a potential vaccine against *T. cruzi* in domestic animals [35]. Subsequently, it is important to study the transmission dynamics of *T. rangeli*, and thus the subsequent linkage with Chagas disease.

Vertebrate hosts do not necessarily experience a significant reduction in fitness due to either the *T. rangeli* parasite infection or from feeding by triatomine bugs. It is reported that *T. rangeli* is pathogenic to triatomine bugs, as opposed to *T. cruzi* [25]. Specifically, infection of *T. rangeli* alters the behavior of *R. prolixus*, which gives rise to the reduction of the volume of successful sucked blood meals. Induced by the loss of nutritional status, the vectors possess lower fitness that leads to decrease of the fecundity and increase of the death of the infected counterparts, and it also has a significant effect on parasite development in the body of vectors which ultimately results in the decrease of infection rate with *T. cruzi* [10,25]. Understanding the behavior changes of *R. prolixus* due to *T. rangeli* infection is of importance since the triatomine infected with *T. rangeli* has lower fitness that could reduce the risk of *T. cruzi* transmission in a given triatomine population.

Like *T. cruzi*, the common host infection with *T. rangeli* takes place in vector feces or urine after feeding of infected bugs, and the healthy vectors could become infected if they are biting with the infected hosts and ingesting the parasites into the bloodstream at this moment [32]. In addition to the typical insect-host-insect systemic transmission, the transmission of *T. rangeli* has an additional route of insect-to-insect co-feeding transmission in the sense that susceptible bugs can become infected when they are feeding with infected bugs on the same vertebrate hosts [36]. There are increasing evidences to show that co-feeding bugs could spread the parasites in the skin vasculature from infected bugs where co-feeding could reach, since their feeding mechanism includes frequent reversal of the ingestion pump [37–39]. It has also been documented that both competent and quasi-competent hosts are able to serve as intermediate carriers to deliver the parasites between co-feeding insects [36].

The co-feeding transmission route has been noted for many vector-borne diseases in general and tick-borne diseases in particular [40,41]. Some mathematical models have been recently developed by incorporating both systemic and co-feeding transmission routes to study the dynamics of tick-borne disease transmission [42,43], however mathematical modelling study for the co-feeding transmission of parasite *T. rangeli* in the content of Chagas disease spread has not been conducted to the best of our knowledge. Despite intensive efforts in understanding the transmission process of Chagas disease, it remains unclear how the insect-to-insect co-feeding transmission and the pathogenicity of *T. rangeli* induced behavior changes of triatomine vectors impact the risk of Chagas disease transmission.

Our focus in this study is to derive a novel mathematical model to explore the interaction among triatomine bugs, e.g., *R. prolixus*, competent and quasi-competent vertebrate hosts and parasites of *T. rangeli*. The transmission routes incorporated in the model include not only the normal systemic transmission, but also the insect-to-insect co-feeding transmission with additional attention on the pathogenicity to the vectors. We also conduct a qualitative analysis for the long-term dynamical behavior of the proposed model with an emphasis on the influence on long-term behaviors of the co-feeding transmission and pathogenicity to vectors. This qualitative analysis should provide useful insights to inform more integrated insect-borne disease intervention strategies.

2. Model development and formulation

2.1. Model development

To model the *T. rangeli* parasite transmission dynamics among triatomine bugs, competent and quasi-competent hosts, we make certain assumptions. The first is that all triatomine bugs and their hosts are assumed homogeneous mixing, and their total population sizes are assumed to change with time for triatomine bugs, while constants for both competent and quasi-competent hosts. Competent hosts (e.g., humans and dogs) have the ability to deliver parasites via both systemic and co-feeding transmission mechanisms, whereas quasi-competent hosts (e.g., chickens) only possess the ability of co-feeding transmission route. Triatomine bugs infecting with *T. rangeli* have a lower fitness that leads to the reduction of fecundity and parasite-induced death, while the *T. rangeli* infection on hosts does not alter their demography as their birth and death, and their contact behavior are also independent of the infection status. Moreover, once hosts and vectors are infected with the parasites, they remain infectious for the rest of their lives.

In our model, both competent hosts and triatomine bugs are therefore divided into susceptible and infected sub-populations denoted by S_j and $I_j\,(j = h, v)$, where subscripts h and v represent competent hosts and vectors, respectively. We assume a constant recruitment rate Λ_h per unit time is added into the susceptible competent host population growth, and both competent hosts and triatomine bugs decay due to their natural death with constant rates μ_h and μ_v, respectively.

In general, the change of each sub-population is determined by their respective birth/recruitment, death and mutual infection which is described as

$$\begin{aligned} S_h' &= \Lambda_h - \lambda_h(t) - \mu_h S_h, \\ I_h' &= \lambda_h(t) - \mu_h I_h, \\ S_v' &= b_v(t) - \lambda_v(t) - \lambda_c(t) - \mu_v S_v, \\ I_v' &= \lambda_v(t) + \lambda_c(t) - d_v I_v - \mu_v I_v, \end{aligned} \tag{1}$$

where $\lambda_h(t)$ and $\lambda_v(t)$ are the infection rates of susceptible competent hosts and susceptible vectors through the systemic transmission after bugs' biting, respectively; $\lambda_c(t)$ is the infection rate of susceptible bugs through the co-feeding transmission, wherein both susceptible and infected bugs are co-feeding on the same competent or quasi-competent hosts; $b_v(t)$ is the birth rate of susceptible triatomine bugs which is influenced by the pathogenic effect on the behavior of triatomine bugs,

and d_v is the parasite-induced death rate of infected vectors due to the pathogenic effect. The specific expressions of $\lambda_h(t)$, $\lambda_v(t)$, $\lambda_c(t)$ and $b_v(t)$ are described below.

Since we are concerned mainly about the long-term behavior of model (1), adding the first and second equations leads to the change of total competent host population $N_h(t) = S_h(t) + I_h(t)$ as

$$N_h'(t) = (S_h(t) + I_h(t))' = \Lambda_h - \mu_h N_h(t).$$

We can obtain

$$\lim_{t\to\infty} N_h(t) = \frac{\Lambda_h}{\mu_h} := N_h.$$

implying the asymptotic total number of competent hosts is constant that we treat it as N_h in the following. Accordingly, the dynamics of competent host population is reduced to one equation as

$$I_h'(t) = \lambda_h(t) - \mu_h I_h(t),$$

and time evolution of susceptible competent host population is determined by

$$S_h(t) = N_h - I_h(t).$$

Pathogenicity to the demography of triatomine bugs Following the work in [16,44], Ricker's type function $b(x) = rxe^{-\sigma x}$ is used to model the reproduction rate of *T. prolixus*, where r is the maximal number of offsprings that a triatomine bug can produce per unit time, σ measures the strength of density dependence. That is, population size increases at the low level density, reaches the carrying capacity because of limited environmental source and then the rate becomes small after that. Moreover, as mentioned in the introduction, the infection with *T. rangeli* can alter the behavior of *R. prolixus* resulting in the reduction of the fecundity and fertility and the increase of the infected pairs' death [10], we therefore have

$$b_v(t) = r(S_v + \theta I_v)e^{-\sigma(S_v+I_v)}$$

to model the birth of susceptible bugs, here $\theta \in [0, 1]$ is the reduction of fecundity and fertility due to *T. rangeli* infection.

Infection rates through systemic transmission To describe $\lambda_h(t)$ and $\lambda_v(t)$, we denote by N_q the total number of quasi-competent hosts which are blood providers for triatomine bugs, while are not involved in the systemic transmission. Due to the behavior and environmental conditions of triatomine species, their host-feeding patterns show wide variability, we thus denote by α the biting preference of quasi-competent hosts in relative to competent hosts [14,26,45]. Denote a by the total number of bites per bug per unit time, then the average number of infected bites per competent host per unit time is $\frac{aI_v(t)}{N_h+\alpha N_q}$. Since the bites given by vectors are equal to those received by their hosts, the total number of infected bites received by all competent susceptible hosts per unit time is $\frac{aI_v(t)}{N_h+\alpha N_q}S_h(t)$. Let b be the transmission proportion of susceptible bugs getting infected per bite, then the infection rate of susceptible hosts is

$$\lambda_h(t) = b\frac{aI_v(t)}{N_h + \alpha N_q}S_h(t) := \beta_h I_v(t)S_h(t),$$

where

$$\beta_h = b\frac{a}{N_h + \alpha N_q} \tag{2}$$

is the transmission rate from infected bugs to susceptible competent hosts.

Let c be the transmission proportion of susceptible bugs getting infected per bite, the infection rate $\lambda_v(t)$ can be similarly determined as

$$\lambda_v(t) = c\frac{aS_v(t)}{N_h + \alpha N_q}I_h(t) := \beta_v S_v(t)I_h(t),$$

where

$$\beta_v = c\frac{a}{N_h + \alpha N_q}. \tag{3}$$

Infection rate through co-feeding transmission It is crucial to characterize the infection rate $\lambda_c(t)$ through insect-to-insect co-feeding transmission. Since both competent and quasi-competent hosts are able to act as vehicles or carriers to transport the *T. rangeli* parasites during co-feeding transmission mechanism, $\lambda_c(t)$ consists of two components, i.e.,

$$\lambda_c(t) = \lambda_{ch}(t) + \lambda_{cq}(t),$$

where $\lambda_{ch}(t)$ and $\lambda_{cq}(t)$ are the infection rates when both susceptible and infected vectors feed on the same competent or quasi-competent host, respectively.

On the average level, at each competent host, the numbers of bites given by susceptible and infected bugs per unit time are

$$\frac{aS_v(t)}{N_h + \alpha N_q} \quad \text{and} \quad \frac{aI_v(t)}{N_h + \alpha N_q},$$

respectively. We count the numbers of susceptible and infected bugs simultaneously feeding on a competent host at unit time, which are not equivalent to the number of bites given by these two kinds of bugs. This is because of un-equality of bugs' feeding time and unit time. For example, assume the feeding time per bite of bugs be 15 min on a host, and the unit time is one day (24 h), thus we have unit time $\omega = 24 \times 60$ min, accordingly a bite should be equivalent to the average number of bugs as $15/(24 \times 60)$ at unit time.

Accordingly, let τ_1 be the feeding time per bite of bugs on competent hosts, thus a bite on a competent host is equivalent to $\tau_1/(\delta\omega)$ number of bugs at the unit time (ω), and δ is to denote the ratio of night to day. Then, the average numbers of susceptible and infected bugs per unit time during night on a competent host are

$$\frac{aS_v(t)}{N_h + \alpha N_q}\frac{\tau_1}{\delta\omega} \quad \text{and} \quad \frac{aI_v(t)}{N_h + \alpha N_q}\frac{\tau_1}{\delta\omega},$$

respectively. Let β_{ch} be the rate at which susceptible bugs become infected by infected bugs on the same hosts through the co-feeding transmission. Using bilinear incidence, the infection rate between susceptible and infected bugs on a host is

$$\beta_{ch}\frac{aS_v(t)}{N_h + \alpha N_q}\frac{\tau_1}{\delta\omega}\cdot\frac{aI_v(t)}{N_h + \alpha N_q}\frac{\tau_1}{\delta\omega}.$$

We now transform the infection rate from the night time to the unit time on the average level. During the night time $[0, \delta\omega]$, the cumulative infection rate on an average competent host is

$$\int_0^{\delta\omega} \beta_{ch}\frac{aS_v(t)}{N_h + \alpha N_q}\frac{\tau_1}{\delta\omega}\cdot\frac{aI_v(t)}{N_h + \alpha N_q}\frac{\tau_1}{\delta\omega}\,dt.$$

Hence, averaging at the unit time length ω leads to the average infection rate on a competent host as

$$\frac{1}{\omega}\int_0^{\delta\omega} \beta_{ch}\frac{aS_v(t)}{N_h + \alpha N_q}\frac{\tau_1}{\delta\omega}\cdot\frac{aI_v(t)}{N_h + \alpha N_q}\frac{\tau_1}{\delta\omega}\,dt.$$

We further assume the number of bugs feeding on the hosts are the same at the short unit time, the infection rate via insect-to-insect transmission at unit time on an average competent host is given by

$$\frac{1}{\omega}\int_0^{\delta\omega} \beta_{ch}\frac{aS_v}{N_h + \alpha N_q}\frac{\tau_1}{\delta\omega}\cdot\frac{aI_v}{N_h + \alpha N_q}\frac{\tau_1}{\delta\omega}\,dt \approx \frac{1}{\delta}\beta_{ch}\frac{aS_v}{N_h + \alpha N_q}\frac{\tau_1}{\omega}\cdot\frac{aI_v}{N_h + \alpha N_q}\frac{\tau_1}{\omega}.$$

Thus the total insect-to-insect infection rate at all competent hosts per unit time is

$$\lambda_{ch}(t) = \frac{1}{\delta}\beta_{ch}N_h\left(\frac{a}{N_h + \alpha N_q}\frac{\tau_1}{\omega}\right)^2 S_v(t)I_v(t) := \hat{\beta}_{ch}S_v(t)I_v(t),$$

where we have defined

$$\hat{\beta}_{ch} = \frac{1}{\delta}\beta_{ch}N_h\left(\frac{a}{N_h + \alpha N_q}\frac{\tau_1}{\omega}\right)^2. \tag{4}$$

Similarly, denote by τ_2 the feeding time per bite of bugs on quasi-competent hosts, and β_{cq} the rate at which susceptible bugs become infected by infected bugs on the same quasi-competent hosts through the co-feeding transmission. Accordingly, the infection rate of susceptible bugs on all quasi-competent hosts through co-feeding transmission per unit time is

$$\lambda_{cq}(t) = \hat{\beta}_{cq}S_v(t)I_v(t),$$

where

$$\hat{\beta}_{cq} = \frac{1}{\delta}\beta_{cq}N_q\left(\frac{a\alpha}{N_h + \alpha N_q}\frac{\tau_2}{\omega}\right)^2. \tag{5}$$

Accordingly, we have

$$\lambda_c(t) = \lambda_{ch}(t) + \lambda_{cq}(t) = (\hat{\beta}_{ch} + \hat{\beta}_{cq})S_v(t)I_v(t) := \beta_c S_v(t)I_v(t),$$

where

$$\beta_c = \hat{\beta}_{ch} + \hat{\beta}_{cq} \tag{6}$$

is the total infection rate through co-feeding transmission between susceptible and infected bugs interplay transported by both competent and quasi-competent hosts.

In summary, the complex dynamics for the interaction among triatomine bugs, competent/quasi-competent hosts and *T. rangeli* parasites are described by the following differential equations:

$$\begin{cases} I_h'(t) = & \beta_h(N_h - I_h(t))I_v(t) - \mu_h I_h(t), \\ S_v'(t) = & r(S_v(t) + \theta I_v(t))e^{-\sigma(S_v(t)+I_v(t))} - \beta_v S_v(t)I_h(t) - \beta_c S_v(t)I_v(t) - \mu_v \\ & S_v(t), \\ I_v'(t) = & \beta_v S_v(t)I_h(t) + \beta_c S_v(t)I_v(t) - (d_v + \mu_v)I_v(t), \end{cases} \tag{7}$$

where all the parameters involved are non-negative, their biological explanations and ranges are presented in Table 1. The schematic diagram of model (7) is illustrated in Fig. 1.

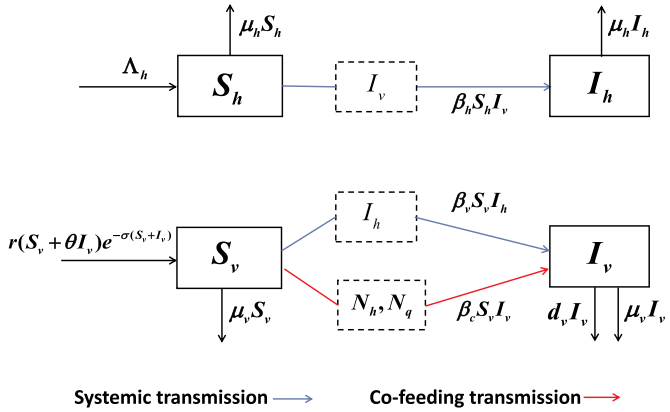

Fig. 1. The flowchart of model (7) involving systemic and co-feeding transmission routes and pathogenic effect on triatomine bugs. Both triatomines and competent host populations are described by SI model. Susceptible competent hosts can get infected through systemic transmission alone, while susceptible vectors can get infected through both systemic and co-feeding transmissions. For the triatomine population, there are the fecundity reduction θ and parasite-induced death rate d_v due to pathogenic effect.

The solution of system (7) is biologically meaningful as the next result shows.

Proposition 1. *System (7) with initial value lying in*

$$\Omega := \{(I_h, S_v, I_v) \in \mathbb{R}^3_+ : I_h \le N_h\}$$

has a unique, non-negative, bounded solution which exists for all $t \ge 0$.

Proof. The above claim directly follows from Theorem 5.2.1 in [48] that system (7) admits a unique nonnegative solution $(I_h(t), S_v(t), I_v(t))$ through an initial value $(I_h(0), S_v(0), I_v(0)) \in \Omega$ with the maximal interval of existence $[0, T)$ for some $T > 0$. It remains to prove the boundedness which also implies the global existence of the solution.

It is clear that $I_h \le N_h$. Adding the second and third equations together in system (7) gives

Table 1
Parameter description and justification.

Parameter	Description	Range/value	Reference/Justification
N_h	total number of competent hosts	varied	human and dogs et al. are considered as in [3]
N_q	total number of quasi-competent hosts	varied	birds and poultry such as chicken are considered as in [3]
α	biting preference of quasi-competent hosts to competent hosts	$(0, \infty)$	wide variability depending upon the opportunistic behavior and variable ecological, biological and social contexts of triatomine species [14,26]
a	number of bites per bug per unit time	[0.2, 33]/day	bites of *R. prolixus* on hosts suggested from [45]
b	transmission probability from infected bugs to susceptible competent hosts per contact	[0.00271,0.06]	human and dogs are suggested as those competent hosts as in [3,8]
c	transmission probability from infected competent hosts to susceptible bugs per contact	[0.00026,0.49]	human and dogs are considered as those in [8,12]
μ_h	per capita mortality rate of competent hosts	[0.000038,0.0025]/day	human, dogs are suggested in this study [8,12]
μ_v	per capita mortality rate of vectors	[0.0045,0.0083]/day	corresponding to a life expectancy of 120–220 days [8,12]
r	the maximal number of offsprings that a triatomine bug can produce per unit time	[0.0274,0.7714]/day	corresponding to those values from [3,12,46]
σ	density-dependency strength measuring the reproduction of bugs	$(0, \infty)$	assumed in this study
θ	reproduction reduction of bugs due to the infection	[0,1]	a scalar term that infected vectors had slightly lower fitness than uninfected vectors
ω	unit time	1 day	simulation designed
$\tau_1(\tau_2)$	feeding time per bite on a competent (quasi-competent) host	10–15 min	short and frequent feeding time comparing the tick population [9]
δ	ratio of night to unit time	0.5	assumed in this study
β_{ch}	transmission rate from infected bugs to susceptible bugs on an average competent host during night	0.005	similar scale suggested as β_v due to limited knowledge of co-feeding transmission from [36]
β_{cq}	transmission rate from infected bugs to susceptible bugs on an average quasi-competent host during night	$\beta_{ch}/5$	assumed, based on the limited information on [36], where around one fifth comparing the transmission on competent host
d_v	*T. rangeli* parasite-induced per capita mortality rate of infected bugs	[0.0188,0.0347]/day	estimated from [47], see subsection 2.2

Table 2
Equilibria and their stability of the model (7).

$\mathcal{R}_v < 1$		$E_v = (0, 0, 0)$	stable
$\mathcal{R}_v > 1$	$\mathcal{R}_0 < 1$	$E_v = (0, 0, 0)$	unstable
		$E_0 = (0, \frac{1}{\sigma}\ln\mathcal{R}_v, 0)$	stable
	$\mathcal{R}_0 > 1$	$E_v = (0, 0, 0)$	unstable
		$E_0 = (0, \frac{1}{\sigma}\ln\mathcal{R}_v, 0)$	unstable
		$E^* = (I_h^*, S_v^*, I_v^*)$	stable under some sufficient conditions

$$(S_v + I_v)'(t) \le r(S_v(t) + I_v(t))e^{-\sigma(S_v+I_v)} - \mu_v(S_v(t) + I_v(t)) \le \frac{r}{\sigma e} - \mu_v(S_v(t) + I_v(t))$$

because of $xe^{-\sigma x} \le 1/(\sigma e)$ if $x > 0$. This immediately yields

$$\limsup_{t\to\infty}(S_v + I_v) \le \frac{r}{\mu_v}\frac{1}{\sigma e}$$

implying the boundedness of S_v and I_v subject to the initial constraints. □

2.2. Model parameter estimation

We here estimate the parasite-induced death rate per triatomine bug d_v. According to Table 2 in [47] for triatomine species *R. prolixus*, the ratio of mortalities between *T. rangeli*-infected and uninfected bugs is reported as 19.45:3.75. Adopting this ratio, we have

$$(d_v + \mu_v)/\mu_v = 19.45/3.75,$$

which leads to

$$d_v = 4.1867 \times \mu_v \in [0.0188, 0.0347]/day,$$

where we use the values of μ_v in Table 1.

Moreover, due to the limited knowledge of *T. rangeli* transmission probabilities between hosts and bugs and among bugs, the parameter values of b, c, β_{ch} and β_{cq} are based on those of both parasites *T. cruzi* and *T. rangeli* in the literature. The justification of other parameter estimations is provided in Table 1. Differences in parameter values may result in quantitative differences in model solutions, while the qualitative analysis remains valid.

3. Results

3.1. Dynamics of vector-free equilibrium

It is obvious that system (7) has a vector-free equilibrium $E_v = (0, 0, 0)$. The Jacobian matrix at E_v is

$$J(E_v) = \begin{pmatrix} -\mu_h & 0 & \beta_h N_h \\ 0 & r - \mu_v & \theta r \\ 0 & 0 & -(d_v + \mu_v), \end{pmatrix},$$

and the corresponding eigenvalues are $-(d_v + \mu_v)$, $-\mu_h$ and $r - \mu_v$. Denote

$$\mathcal{R}_v = \frac{r}{\mu_v},$$

then it is a threshold which characterizes the persistence or extinction of vector population in the long time dynamics. Utilizing the comparison principle and theory of monotone dynamical systems [48], the following result is obtained.

Theorem 2. *For model (7), vector-free equilibrium E_v is globally asymptotically stable if $\mathcal{R}_v < 1$ and unstable if $\mathcal{R}_v > 1$.*

Proof. In the case of $\mathcal{R}_v > 1$, the eigenvalue of $r - \mu_v$ is positive indicating E_v unstable. In the case of $\mathcal{R}_v < 1$, then all the three eigenvalues for the linearized system at vector-free equilibrium are real and negative implying E_v locally asymptotically stable.

Let $N_v = S_v + I_v$ and adding the second and third equations of system (7) yields

$$N_v' \le rN_v e^{-\sigma N_v} - \mu_v N_v \le (r - \mu_v)N_v.$$

Solving above inequality with any feasible initial value $N_v(0) = S_v(0) + I_v(0)$, we have

$$\limsup_{t\to\infty} N_v(t) \le \lim_{t\to\infty} N_v(0)e^{\mu_v(\mathcal{R}_v-1)t} = 0$$

when $\mathcal{R}_v < 1$. That is, the solutions of S_v and I_v with any feasible initial condition will tend to zero provided that $\mathcal{R}_v < 1$. Moreover, for the subsystem of I_h, it is cooperative with its positive invariance set $[0, N_h]$. Furthermore, it is clear that E_v is a unique single equilibrium of system (7) for $\mathcal{R}_v < 1$. Following the Theorem 3.2.2 in [48], any solution of $I_h(t)$ for $t \ge 0$ starting on the domain $[0, N_h]$ is monotone and converges to equilibrium. Thus, E_v is a global attractive equilibrium which indicates it is globally asymptotically stable if $\mathcal{R}_v < 1$. □

3.2. T. rangeli basic reproduction number

The condition of $\mathcal{R}_v > 1$ is always assumed in the following. The system (7) has a parasite-free equilibrium

$$E_0 = (0, S_v^0, 0) \quad \text{and} \quad S_v^0 = \frac{1}{\sigma}\ln\mathcal{R}_v > 0.$$

Following the next generation matrix method [49], we define the new infection matrix

$$F = \begin{pmatrix} 0 & \beta_h N_h \\ \beta_v S_v^0 & \beta_c S_v^0 \end{pmatrix}$$

and the transition matrix

$$V = \begin{pmatrix} \mu_h & 0 \\ 0 & d_v + \mu_v \end{pmatrix}.$$

Subsequently, the basic reproduction number of the model (7), is defined as the spectral radius of the next generation matrix FV^{-1}, namely,

$$\mathcal{R}_0 = \rho(FV^{-1}) = \frac{1}{2}(\mathcal{R}_{vv} + \sqrt{(\mathcal{R}_{vv})^2 + 4\mathcal{R}_{hv}^2}), \tag{8}$$

where

$$\mathcal{R}_{vv} = \frac{\beta_c S_v^0}{d_v + \mu_v} \quad \text{and} \quad \mathcal{R}_{hv} = \sqrt{\frac{\beta_h N_h}{\mu_h}\frac{\beta_v S_v^0}{d_v + \mu_v}}.$$

In fact, $\mathcal{R}_{vv}$ is the expected number of new infections induced by direct insect-to-insect co-feeding transmission in vector's average lifespan, while $\mathcal{R}_{hv}$ is the expected number of new infections induced by indirect vector-host-vector transmission, where an infected insect bites susceptible hosts which leads to susceptible hosts get infected, and then propagate the infection to the next new bug generation. Moreover, it is easy to check the following equivalence:

$$\mathcal{R}_0 < 1 \Longleftrightarrow \mathcal{R}_{vv} + \mathcal{R}_{hv}^2 < 1. \tag{9}$$

Following Theorem 2 in [49], we obtain the dynamical behavior of the parasite-free equilibrium E_0.

Theorem 3. *With $\mathcal{R}_v > 1$, the parasite-free equilibrium E_0 of model (7) is locally asymptotically stable if $\mathcal{R}_0 < 1$ and unstable when $\mathcal{R}_0 > 1$.*

3.2.1. The effect of host community composition on $\mathcal{R}_0$

The host community composition is commonly considered as an important factor on the risk of vector-borne infection. Fig. 2 shows the influence of triatomine bugs' biting preference α, numbers of competent

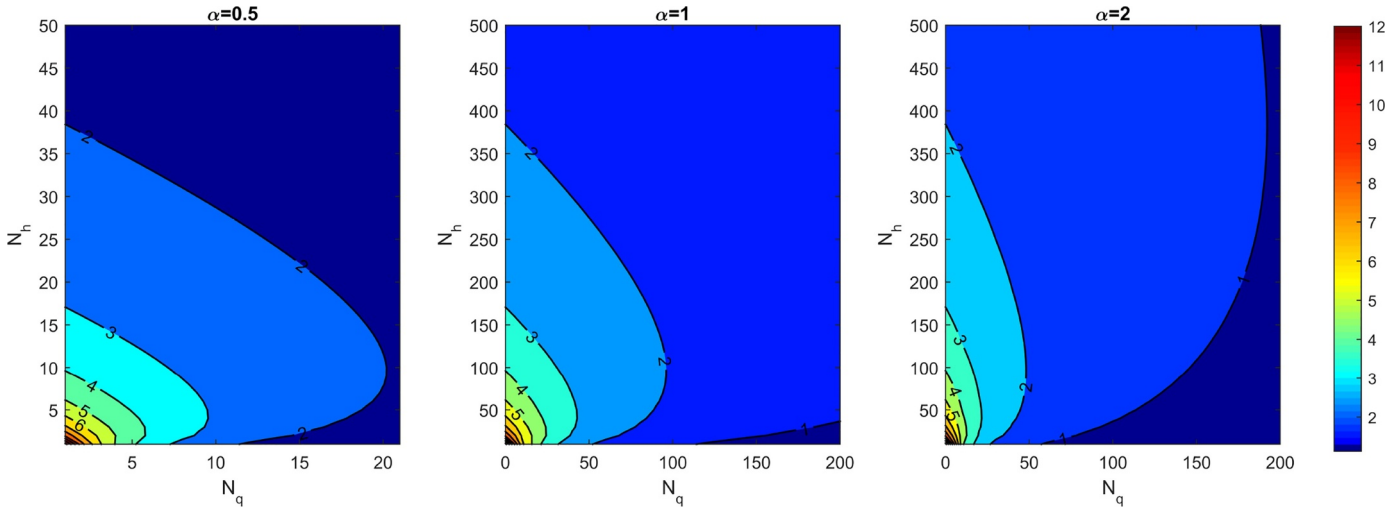

Fig. 2. Contour plots of the basic reproduction number $\mathcal{R}_0$ versus N_h, N_q and α. In these simulations, $N_h \in [10, 500]$, $N_q \in [0, 200]$ and $\alpha = 0.5, 1, 2$, and others are $a = 0.6$, $b = 0.06$, $c = 0.49$, $r = 0.0274$, $\mu_h = 0.0025$, $\mu_v = 0.0083$, $\sigma = 0.1$, $\theta = 0.9$, $\omega = 1$, $\tau_1 = \tau_2 = 15/60/24$, $\delta = 0.5$, $\beta_{ch} = 0.005$, $\beta_{cq} = 0.001$, $d_v = 0.0246$.

hosts N_h and quasi-competent hosts N_q on the basic reproduction number $\mathcal{R}_0$. We observe that $\mathcal{R}_0$ is sensitive to the vectors' biting preference α, and a smaller α allows a wider range of quasi-competent host N_q to maintain the same level of $\mathcal{R}_0$ as indicated by contours of $\mathcal{R}_0 = 2$ in Fig. 2. Moreover, by varying N_h and N_q, the values of $\mathcal{R}_0$ can change from below 1 to above as shown in Fig. 2(b and c), implying the change from extinction to persistence of *T. rangeli* parasite infection.

Fig. 3 (a and b) particularly illustrate the respective dependence of $\mathcal{R}_0$ on N_h and N_q in the case of $\alpha = 1$. With the increase of N_h as shown in Fig. 3(a), we notice that $\mathcal{R}_0$ increases initially, peaks then at a certain value of N_h, and declines afterward until less than 1. This implies that the increase of the number of competent hosts does not necessarily lead to the increase of $\mathcal{R}_0$; indeed, either a small or large size of competent host population could lead to $\mathcal{R}_0 < 1$ which indicates the extinction of *T. rangeli* parasite infection. By contrast, Fig. 3(b) shows that $\mathcal{R}_0$ is a monotonically decreasing function of N_q and finally tends to below 1. Biologically, this indicates that the increase of quasi-competent hosts can eventually result in the extinction of *T. rangeli* parasite infection.

As $\mathcal{R}_0$ depends on β_c, which is an important parameter and its expression is an integrated combination of N_h, N_q and α (Eqs. (4)–(6)), we further examine the dependence of β_c on host populations. As shown in Fig. 3(c and d), similar profiles as those in Fig. 3(a and b) are observed. This indicating that β_c plays an important role in the non-monotonic behavior of $\mathcal{R}_0$ on N_h.

3.2.2. The role of $\mathcal{R}_{hv}$ and $\mathcal{R}_{vv}$

In this subsection, we show the relative contributions of $\mathcal{R}_{vv}$ and $\mathcal{R}_{hv}$ on the basic reproduction number $\mathcal{R}_0$. In Fig. 4, the first two columns show the contribution of $\mathcal{R}_{vv}$ and $\mathcal{R}_{hv}$ to $\mathcal{R}_0$ in terms of competent hosts N_h and quasi-competent hosts N_q, for $\alpha = 0.1, 1, 10$, respectively, and the third column shows the dependence of $\mathcal{R}_0$ on the same chosen parameters. We observe that the ratio $\mathcal{R}_{vv}/\mathcal{R}_0$ is extremely small and $\mathcal{R}_{hv}/\mathcal{R}_0$ is close to unity. These imply that the systemic transmission plays a more significant role than co-feeding transmission on $\mathcal{R}_0$, and

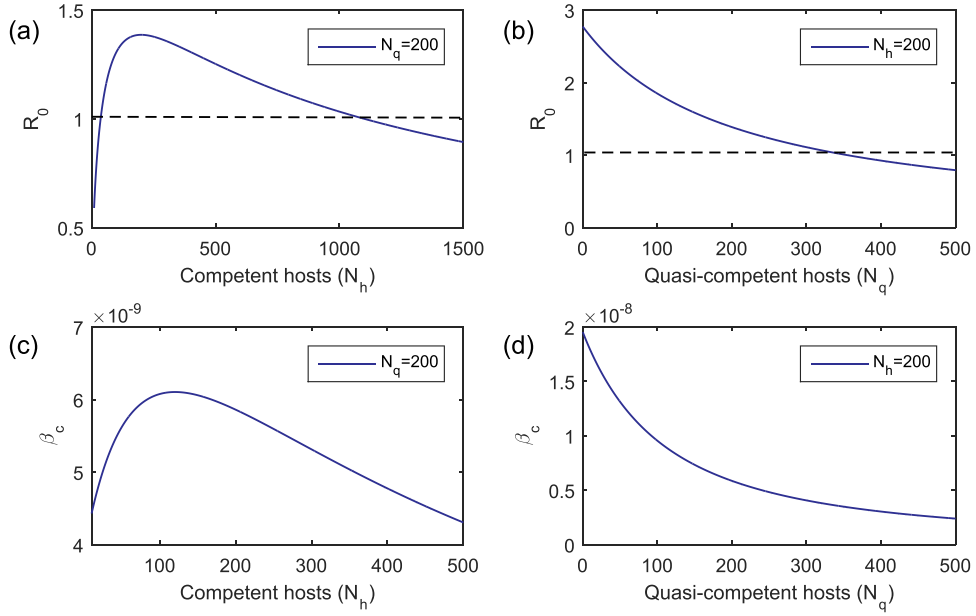

Fig. 3. The relationship of basic reproduction number $\mathcal{R}_0$ and co-feeding transmission rate β_c with respect to competent hosts N_h and quasi-competent hosts N_q. (a) $\mathcal{R}_0$ vs. $N_h \in [10, 1500]$ and $N_q = 200$; (b) $\mathcal{R}_0$ vs. $N_q \in [0, 500]$ and $N_h = 200$; (c) β_c vs. $N_h \in [10, 500]$ and $N_q = 200$; (d) β_c vs. N_q, and $N_h = 200$. Others are $\alpha = 1$, $a = 0.6$, $b = 0.06$, $c = 0.49$, $r = 0.0274$, $\mu_h = 0.0025$, $\mu_v = 0.0083$, $\sigma = 0.1$, $\theta = 0.9$, $\omega = 1$, $\tau_1 = \tau_2 = 15/60/24$, $\delta = 0.5$, $\beta_{ch} = 0.005$, $\beta_{cq} = 0.001$, $d_v = 0.0246$.

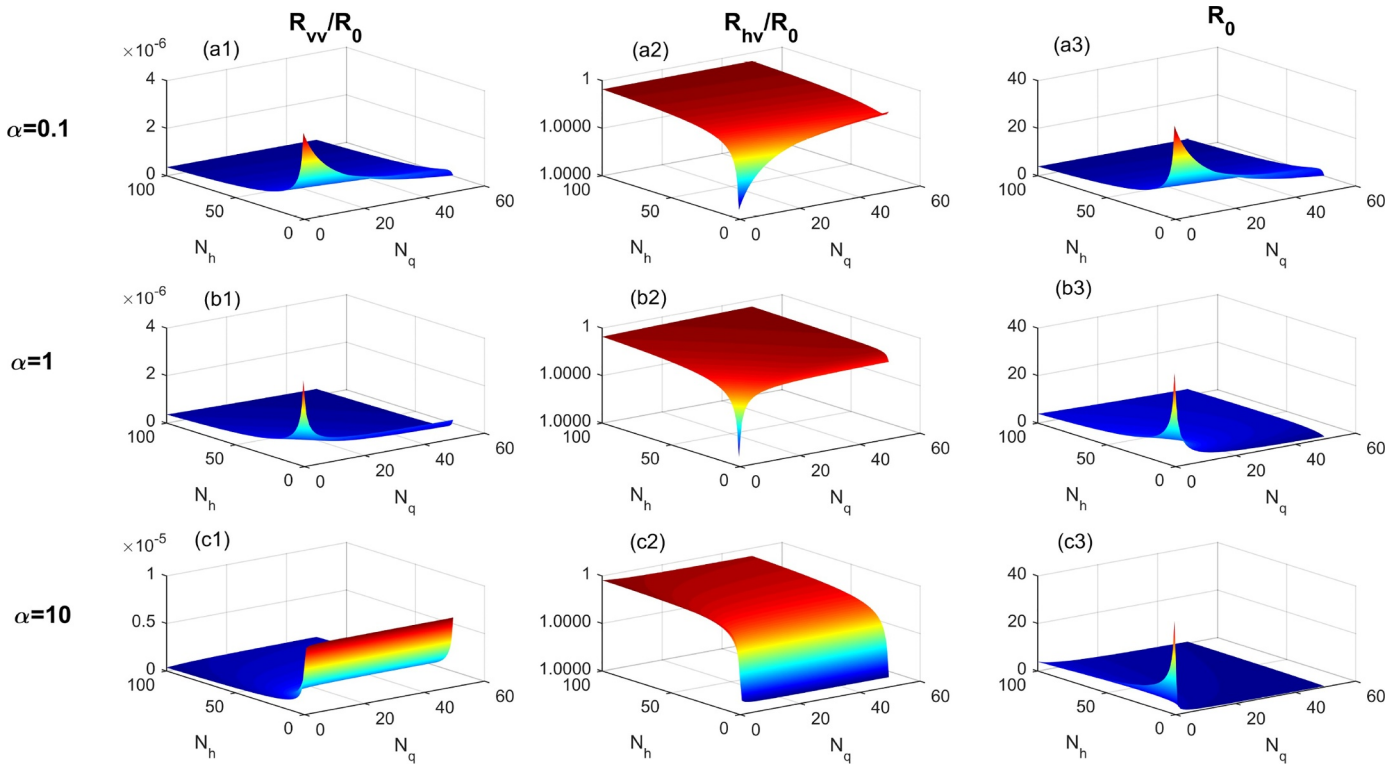

Fig. 4. An illustration of the role of $\mathcal{R}_{vv}$ and $\mathcal{R}_{hv}$ to $\mathcal{R}_0$ with respect to $N_h \in [1, 100]$ and $N_q \in [0, 50]$ and $\alpha = 0.1, 1, 10$. For the panels from top, middle to bottom, α corresponds to 0.1, 1, 10, respectively. Others are $a = 0.6$, $b = 0.06$, $c = 0.49$, $r = 0.0274$, $\mu_h = 0.0025$, $\mu_v = 0.0083$, $\sigma = 0.1$, $\theta = 0.9$, $\omega = 1$, $\tau_1 = \tau_2 = 15/60/24$, $\delta = 0.5$, $\beta_{ch} = 0.005$, $\beta_{cq} = 0.001$, $d_v = 0.0246$.

the value of $\mathcal{R}_0$ is mainly determined by $\mathcal{R}_{hv}$. The α value varies widely, and it influences the value of $\mathcal{R}_0$ in Eq. (8), where β_h, β_v and β_c are related. By increasing α as shown in Fig. 4(a1)–(c1), the contribution of $\mathcal{R}_{vv}$ to $\mathcal{R}_0$ is slightly increased.

3.3. Parasite-positive equilibrium

To study the parasite persistence, seeking for the positive equilibrium of system (7) is required which is summarized as follows. The complete proof is provided in Appendix A.

Theorem 4. *With $\mathcal{R}_v > 1$, the model (7) admits a unique parasite-positive equilibrium $E^* = (I_h^*, S_v^*, I_v^*)$ if and only if $\mathcal{R}_0 > 1$, where I_v^* is determined by*

$$r\left(\frac{g_1 I_v^* + \omega_1}{g_2 I_v^* + \omega_2} + \theta I_v^*\right) e^{-\sigma\left(\frac{g_1 I_v^* + \omega_1}{g_2 I_v^* + \omega_2} + I_v^*\right)} = d_v I_v^* + \mu_v\left(\frac{g_1 I_v^* + \omega_1}{g_2 I_v^* + \omega_2} + I_v^*\right), \tag{10}$$

and

$$g_1 = \beta_h(d_v + \mu_v),\ \ g_2 = \beta_h\beta_c,\ \ \omega_1 = \mu_h(d_v + \mu_v),\ \ \omega_2 = \mu_h\beta_c + \beta_h\beta_v N_h.$$

I_h^* and I_v^* are determined by

$$I_h^* = \frac{\beta_h I_v^*}{\beta_h I_v^* + \mu_h} N_h \quad \text{and} \quad S_v^* = \frac{g_1 I_v^* + \omega_1}{g_2 I_v^* + \omega_2}, \tag{11}$$

respectively.

3.4. Stability of parasite-positive equilibrium

We now present the stability analysis of E^* to show the parasite persistence. To do this, we linearize system (7) at E^* and obtain the characteristic equation

$$f(\lambda) = \lambda^3 + b_2\lambda^2 + b_1\lambda + b_0 = 0. \tag{12}$$

The coefficients are

$$\begin{aligned} b_2 &= -(a_{11} + a_{22} + a_{33}),\\ b_1 &= a_{11}a_{22} + a_{11}a_{33} + a_{22}a_{33} - a_{13}a_{31} - a_{23}a_{32},\\ b_0 &= a_{11}a_{23}a_{32} + a_{13}a_{22}a_{31} - a_{11}a_{22}a_{33} - a_{13}a_{21}a_{32}, \end{aligned} \tag{13}$$

where

$$\begin{aligned} a_{11} &= -(\beta_h I_v^* + \mu_h) < 0,\ \ a_{12} = 0,\ \ a_{13} = \mu_h\tfrac{I_h^*}{I_v^*} > 0,\\ a_{21} &= -\beta_v S_v^* < 0,\\ a_{22} &= -\tfrac{ur(\sigma S_v^*(\theta I_v^* + S_v^*) + \theta I_v^*)}{S_v^*} < 0,\\ a_{23} &= -\beta_c S_v^* - ur\sigma(\theta I_v^* + S_v^*) + ur\theta,\\ a_{31} &= \beta_v S_v^* > 0,\ \ a_{32} = \beta_v I_h^* + \beta_c I_v^* > 0,\ \ a_{33} = -\beta_v S_v^*\tfrac{I_h^*}{I_v^*} < 0, \end{aligned} \tag{14}$$

and

$$u = e^{-\sigma(S_v^* + I_v^*)}.$$

To show that all the characteristic roots of Eq. (12) have negative real parts, our framework is quite general by using the Routh-Hurwitz criteria in the sense that we need to show $b_0 > 0$, $b_1 > 0$, $b_2 > 0$ and $b_1 b_2 > b_0$.

Claim: $b_0 > 0$, $b_1 > 0$ and $b_2 > 0$.

It is easy to see $b_2 = -(a_{11} + a_{22} + a_{33}) > 0$ since all a_{11}, a_{22} and a_{33} are negative. For the term b_1, we firstly get

$$a_{11}a_{22} > 0, \quad a_{11}a_{33} - a_{13}a_{31} = \beta_h\beta_v I_h^* S_v^* > 0, \tag{15}$$

and

$$\begin{aligned} a_{22}a_{33} - a_{23}a_{32} = {} & \frac{ur\sigma(\theta I_v^* + S_v^*)(\beta_v I_h^*(S_v^* + I_v^*) + \beta_c I_v^{*2})}{I_v^*}\\ & + \frac{\beta_c S_v^* I_v^*(d_v + \mu_v(1-\theta))}{\theta I_v^* + S_v^*} > 0. \end{aligned} \tag{16}$$

So we have $b_1 > 0$.

For b_0, we get

$$\begin{aligned} b_0 &= B\sigma + \frac{\beta_c S_v^* I_v^* (\beta_h I_v^* + \mu_h)(d_v + \mu_v(1-\theta))}{\theta I_v^* + S_v^*} + \frac{\beta_v \mu_h I_h^* (\beta_v I_h^* S_v^* + \beta_c S_v^* I_v^* - ur\theta I_v^*)}{I_v^*} \\ &= B\sigma + \frac{\beta_c S_v^* I_v^* (\beta_h I_v^* + \mu_h)(d_v + \mu_v(1-\theta))}{\theta I_v^* + S_v^*} + \frac{\beta_v \mu_h I_h^* S_v^* (d_v + \mu_v(1-\theta))}{\theta I_v^* + S_v^*} \\ &= B\sigma + \frac{S_v^* (d_v + \mu_v(1-\theta))(\beta_c I_v^* (\beta_h I_v^* + \mu_h) + \beta_v \mu_h I_h^*)}{\theta I_v^* + S_v^*} \end{aligned} \tag{17}$$

where

$$B = ur(\theta I_v^* + S_v^*)(\beta_v I_h^* (\beta_h (S_v^* + I_v^*) + \mu_h) + \beta_c I_v^* (\beta_h I_v^* + \mu_h)) > 0. \tag{18}$$

Then we have $b_0 > 0$.

3.4.1. Sufficient conditions for local stability

Though the conditions of $b_0 > 0$, $b_1 > 0$ and $b_2 > 0$ from Eq. (13) have been proved, the condition of $b_1 b_2 > b_0$ is not always satisfied. Additionally, it is not easy to simplify the equivalent condition for $b_1 b_2 > b_0$ because of lack of analytical expression of I_v^*. However, we find some sufficient conditions such that this condition holds. By the Routh-Hurwitz criteria, we have the following results.

Theorem 5. *With $\mathcal{R}_v > 1$ and $\mathcal{R}_0 > 1$, the parasite-positive equilibrium $E^* = (I_h^*, S_v^*, I_v^*)$ is locally asymptotically stable if one of the following conditions is satisfied:*

(a) $2\theta > 1 + \frac{d_v}{\mu_v}$;

(b) $\beta_c < \beta_h \frac{(d_v + \mu_v) - \beta_v N_h}{\mu_h}$ *and* $\beta_c < \beta_h$;

(c) $\frac{2\theta\mu_v}{\mu_v + d_v} + \frac{\beta_h (d_v + \mu_v)}{\beta_h \beta_v N_h + \beta_c \mu_h} > 1$ *and* $\beta_c < \beta_h$.

Proof. To prove the locally asymptotic stability, we need to show that condition of $b_1 b_2 > b_0$. We can write it as

$$b_1 b_2 - b_0 = C_2 \sigma^2 + C_1 \sigma + C_0, \tag{19}$$

where

$$\begin{aligned} C_2 =& \frac{u^2 r^2 (\theta I_v^* + S_v^*)^2 (I_v^* (I_v^* (\beta_h + \beta_c) + \mu_h) + \beta_v I_h^* (S_v^* + I_v^*))}{I_v^*} > 0, \\ C_1 =& \frac{ur}{S_v^{*2} I_v^{*2}} [\beta_v I_h^* I_v^* (\theta I_v^* + S_v^*)(I_v^* (S_v^{*2}(2\beta_h + \beta_c) + ur\theta(S_v^* + I_v^*)) + 2\mu_h S_v^{*2}) \\ &+ I_v^{*2} (I_v^* (\beta_h I_v^* (\theta I_v^* + S_v^*)(\beta_h S_v^* + 2ur\theta) + \beta_c (d_v \\ &S_v^{*2} + ur\theta I_v^* (\theta I_v^* + S_v^*) + \mu_v (1-\theta) S_v^{*2})) \\ &+ 2\mu_h I_v^* (\theta I_v^* + S_v^*)(\beta_h S_v^* + ur\theta) + \mu_h{}^2 S_v^* (\theta I_v^* + S_v^*)) \\ &+ \beta_v^2 I_h^{*2} S_v^{*2} (S_v^* + I_v^*)(\theta I_v^* + S_v^*)] > 0, \end{aligned} \tag{20}$$

and

$$\begin{aligned} C_0 =& \frac{I_v^*}{S_v^{*2}} (\beta_h^2 \beta_v I_h^* S_v^{*3} + ur\theta S_v^* (\beta_h (\beta_h I_v^{*2} + 2\beta_v I_h^* S_v^*) + 2\beta_h \mu_h I_v^* + \mu_h^2) + u^2 \\ &r^2 \theta^2 I_v^* (\beta_h I_v^* + \mu_h)) \\ &+ \frac{\beta_v I_h^* (\beta_c S_v^{*2} (d_v + \mu_v(1-\theta)) + \mu_h \theta I_v^* (d_v + \mu_v)) + \beta_c ur\theta I_v^{*2} (d_v + \mu_v(1-\theta))}{\theta I_v^* + S_v^*} \\ &+ \frac{\beta_h \beta_v^2 I_h^{*2} S_v^{*2}}{I_v^*} + \beta_h \beta_v \mu_h I_h^* S_v^* - \frac{\beta_v \mu_h I_h^* S_v^* (d_v + \mu_v - 2\mu_v \theta)}{\theta I_v^* + S_v^*}. \end{aligned} \tag{21}$$

Thus the last term in (21) is the only possible negative term. A sufficient condition is given by

$$d_v + \mu_v - 2\mu_v \theta < 0 \quad \Leftrightarrow \quad 2\theta > 1 + \frac{d_v}{\mu_v}. \tag{22}$$

Next we will derive the condition (b). We first have

$$\frac{\beta_v \mu_h I_h^* S_v^* (d_v + \mu_v)}{\theta I_v^* + S_v^*} < \beta_v \mu_h I_h^* (d_v + \mu_v) = \beta_c \beta_v I_h^* S_v^* \mu_h + \frac{\beta_v^2 I_h^{*2} S_v^* \mu_h}{I_v^*}, \tag{23}$$

where the last equality is based on the Eq. (A.3). If $\beta_c < \beta_h$, the second last term in (23) can be controlled by the second last term in (21), namely,

$$\beta_c \beta_v I_h^* S_v^* \mu_h < \beta_h \beta_v I_h^* S_v^* \mu_h. \tag{24}$$

Combining the last term in (23) and the third last term in (21) gives

$$\frac{\beta_h \beta_v^2 I_h^{*2} S_v^{*2}}{I_v^*} - \frac{\beta_v^2 I_h^{*2} S_v^* \mu_h}{I_v^*} = \frac{\beta_v^2 I_h^{*2} S_v^*}{I_v^*} (\beta_h S_v^* - \mu_h). \tag{25}$$

Since

$$\beta_h S_v^* = \frac{\beta_h (d_v + \mu_v) I_v^*}{\beta_v I_h^* + \beta_c I_v^*} = \frac{\beta_h (d_v + \mu_v)}{\beta_v \frac{\beta_h N_h}{\beta_h I_v^* + \mu_h} + \beta_c} > \frac{\beta_h (d_v + \mu_v)}{\beta_v \beta_h N_h + \beta_c \mu_h} \mu_h, \tag{26}$$

we get

$$\frac{\beta_h (d_v + \mu_v)}{\beta_v \beta_h N_h + \beta_c \mu_h} > 1 \Rightarrow \frac{\beta_h \beta_v^2 I_h^{*2} S_v^{*2}}{I_v^*} > \frac{\beta_v^2 I_h^{*2} S_v^* \mu_h}{I_v^*}. \tag{27}$$

If we estimate all the last three terms in (21) together, we can get a more relaxed sufficient condition by assuming $\beta_c < \beta_h$. First we rewrite the last term as

$$\begin{aligned} &\frac{\beta_v \mu_h I_h^* S_v^* (d_v + \mu_v - 2\mu_v \theta)}{\theta I_v^* + S_v^*} = \frac{\beta_v \mu_h I_h^* S_v^* (d_v + \mu_v)}{\theta I_v^* + S_v^*} M, \\ &M = 1 - \frac{2\theta\mu_v}{\mu_v + d_v} \le 1. \end{aligned} \tag{28}$$

Then the above derivation applies with only modification of this factor M and provides the following sufficient condition under $\beta_c < \beta_h$

$$\frac{\beta_h (d_v + \mu_v)}{\beta_v \beta_h N_h + \beta_c \mu_h} > M. \tag{29}$$

□

The above results show that, with an emphasis on the pathogenic effect of triatomine bugs, namely the condition of $2\theta > 1 + d_v/\mu_v$ is satisfied, the solution of model (7) converges to the parasite-positive equilibrium E^* when the initial values are close to this equilibrium, and hence the parasite persists. With an emphasis on the co-feeding transmission, the parasite still persists if the following sufficient condition

$$\beta_c < \beta_h \cdot \min\left\{ \frac{(d_v + \mu_v) - \beta_v N_h}{\mu_h}, 1 \right\}$$

is satisfied. By combining the two factors, parasite persistence is guaranteed if the sufficient conditions as shown in case (c) of Theorem 5 are satisfied.

Fig. 5 shows the dynamics of host and bug populations I_h, S_v, I_v and $N_v = S_v + I_v$ of model (7), for different values of N_h. It is shown that all solutions converge to the positive steady states under the conditions $\mathcal{R}_0 > 1$ and $2\theta > 1 + d_v/\mu_v$, as expected. With the increase of N_h, Fig. 5 also shows the change in number of host and bug populations at equilibrium. That is, infected competent host population I_h^* largely increases, susceptible bug population S_v^* largely decreases, infected bug population I_v^* slightly increases and total bug population N_v^* decreases. This is because, with a larger N_h, more susceptible competent hosts S_h contact with I_v which leads to the increase of I_h^*. As such, more susceptible bugs become infected due to the infection between S_v and I_h, giving rise to the decrease of S_v^* and the increase of I_v^*. Nevertheless, I_v^* has a slight increase due to mutual interaction of the infection and additional pathogenic effect. This fact of the large decrease of S_v^* and slight increase of I_v^* leads to the decrease of the birth rate for susceptible bugs and the increase of death rate for infected bugs due to the pathogenic effect, which finally results in the decrease of N_v^* as shown in Fig. 5(d). This scenario could potentially indicate the reduction for the risk of Chagas disease.

Fig. 6 also shows the dynamics of host and bug populations I_h, S_v, I_v

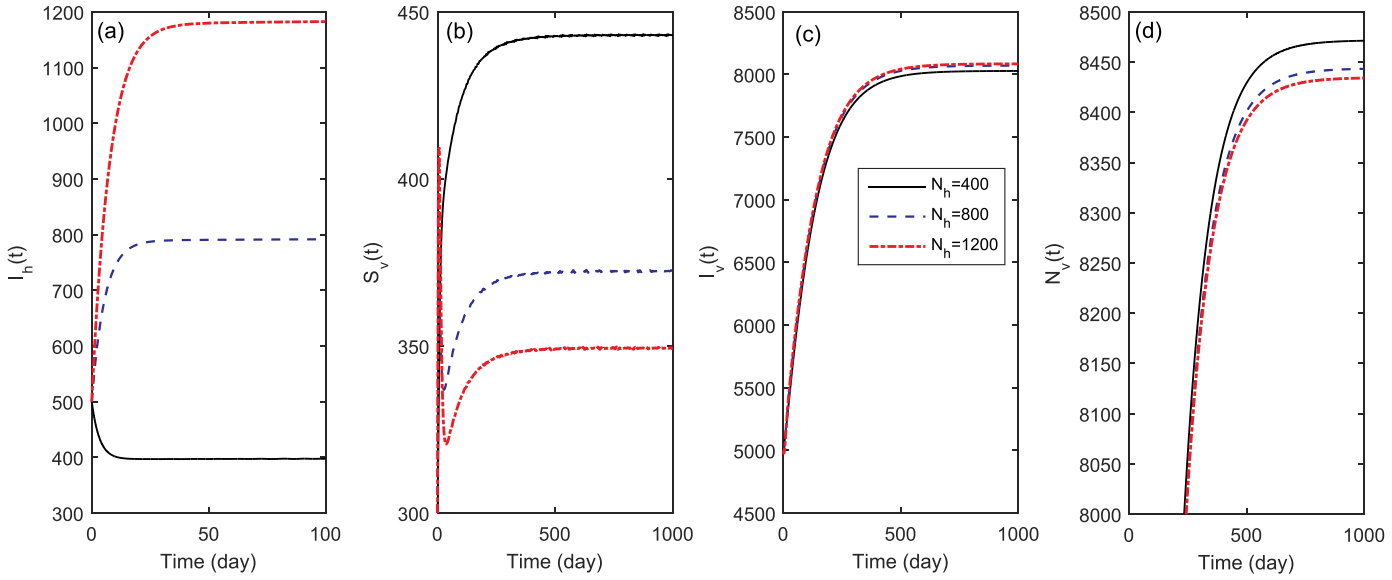

Fig. 5. Time evolution of model solutions when varying N_h from low, median to high, where both $\mathcal{R}_0 > 1$ and $2\theta > 1 + \frac{d_v}{\mu_v}$ are satisfied. (a) $I_h(t)$; (b) $S_v(t)$; (c) $I_v(t)$; (d) $N_v(t) = S_v(t) + I_v(t)$ Here in these simulations, $N_q = 200$, $\alpha = 1$, $a = 0.6$, $b = 0.06$, $c = 0.49$, $\mu_h = 0.0025$, $\mu_v = 0.0083$, $r = 0.0274$, $\sigma = 0.0001$ and $\theta = 0.9$, $\omega = 1$, $\tau = 15/60/24$, $\delta = 0.5$, $\beta_{ch} = 0.005$, $\beta_{cq} = 0.001$, $d_v = 0.00246$.

and $N_v = S_v + I_v$, for different values of N_q. We observe at equilibrium, with the increase of N_q, both I_h^* and I_v^* decrease and both S_v^* and N_v^* increase on the contrary. The main reason is that N_q affects the transmission rates β_h, β_v and β_c, all of which are decreasing functions of N_q. Consequently, with the increase of N_q, less susceptible competent hosts S_h becomes I_h because of smaller β_h which leads to the decrease of I_h^* in Fig. 6(a); less susceptible bugs S_v becomes I_v due to smaller β_v and β_c, leading to the decrease of I_v^* as well in Fig. 6(c). As a consequence of smaller I_v, the pathogenic effect on bugs is less significant, hence larger S_v causes the increase of birth rate of susceptible bugs, therefore the increase of both S_v^* and N_v^* in Fig. 6(b and d). This scenario could potentially indicate the increase for the risk of Chagas disease.

3.4.2. *Special case: without pathogenic effect*

The model (7) analyzed so far shows the locally asymptotic stability of the parasite-positive equilibrium E^*. In general, *T. rangeli* is pathogenic to its insect vectors, however it may not be pathogenic to every triatomine species [35]. Therefore, it is worthwhile to study the dynamics of system (7) in the absence of pathogenic effect on triatomine bugs, i.e., $\theta = 1$ and $d_v = 0$, which allows us to compare both mathematical and biological implications for cases with and without pathogenic effect.

Theorem 6. *With $\mathcal{R}_v > 1$ and $\mathcal{R}_0 > 1$, in the absence of pathogenic effect on triatomine bugs, namely, $\theta = 1$ and $d_v = 0$, system (7) admits a unique parasite-positive equilibrium $E^* = (I_h^*, S_v^*, I_v^*)$ which is globally asymptotically stable.*

Proof. In the case of $\theta = 1$, $d_v = 0$, system (7) reduces to

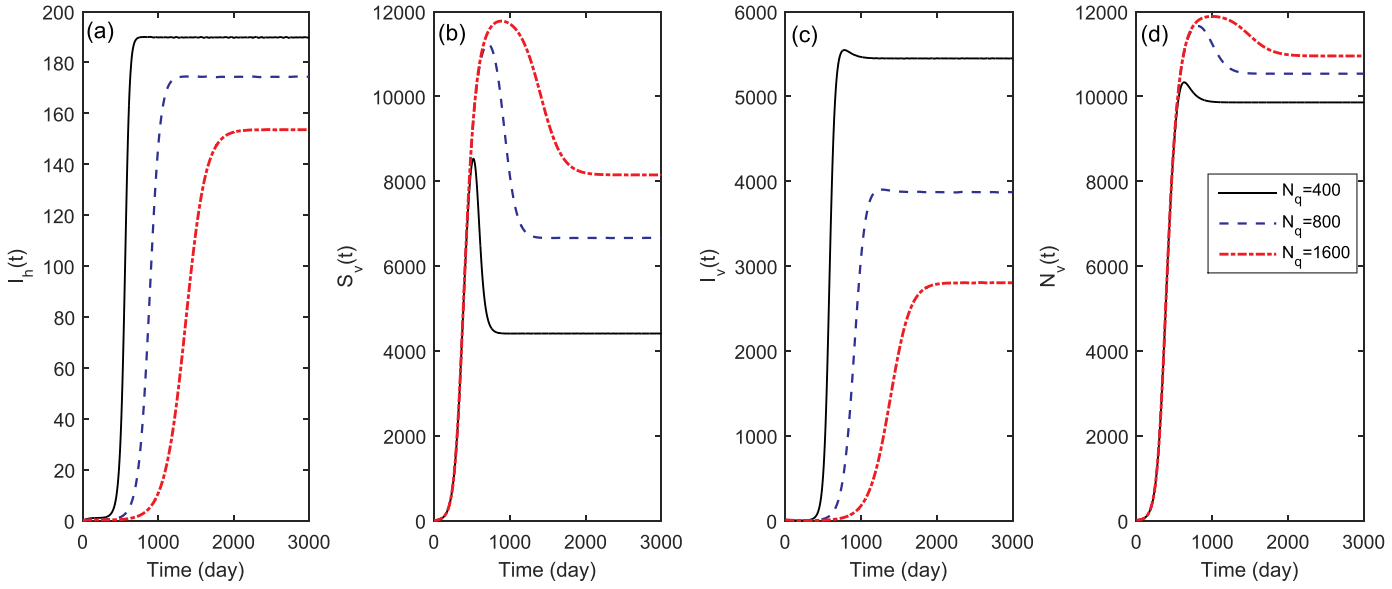

Fig. 6. Time evolution of model solutions when varying N_q from low, median to high, where both $\mathcal{R}_0 > 1$ and $2\theta > 1 + \frac{d_v}{\mu_v}$ are satisfied. (a) $I_h(t)$; (b) $S_v(t)$; (c) $I_v(t)$; (d) $N_v(t) = S_v(t) + I_v(t)$. Here in these simulations, $N_h = 200$, $\alpha = 10$, $a = 0.6$, $b = 0.06$, $c = 0.49$, $\mu_h = 0.0025$, $\mu_v = 0.0083$, $r = 0.0274$, $\sigma = 0.0001$ and $\theta = 0.9$, $\omega = 1$, $\tau = 15/60/24$, $\delta = 0.5$, $\beta_{ch} = 0.005$, $\beta_{cq} = 0.001$, $d_v = 0.00246$.

$$\begin{cases} I_h'(t) = & \beta_h(N_h - I_h(t))I_v(t) - \mu_h I_h(t), \\ S_v'(t) = & r(S_v(t) + I_v(t))e^{-\sigma(S_v(t)+I_v(t))} - \beta_v S_v(t) I_h(t) - \beta_c S_v(t) I_v(t) - \mu_v \\ & S_v(t), \\ I_v'(t) = & \beta_v S_v(t) I_h(t) + \beta_c S_v(t) I_v(t) - \mu_v I_v(t). \end{cases} \tag{30}$$

First of all, it is easy to check that sub-system (30) admits a unique parasite-positive equilibrium $E^* = (I_h^*, S_v^*, I_v^*)$ if $\mathcal{R}_0 > 1$, since it is a special case of system (7).

Adding the second and third equations of system (30), the triatomine bug population satisfies

$$N_v'(t) = rN_v(t)e^{-\sigma N_v(t)} - \mu_v N_v(t). \tag{31}$$

It is obvious that Eq. (31) admits a unique zero equilibrium which is globally asymptotically stable if $\mathcal{R}_v \le 1$, and a unique global attractive equilibrium $N_v^* = S_v^0$ if $\mathcal{R}_v > 1$.

In the case of $\mathcal{R}_v > 1$, the limit system of (30) is reduced to:

$$\begin{cases} I_h'(t) = \beta_h(N_h - I_h(t))I_v(t) - \mu_h I_h(t), \\ I_v'(t) = \beta_v I_h(t)(S_v^0 - I_v(t)) + \beta_c(S_v^0 - I_v(t))I_v(t) - \mu_v I_v(t). \end{cases} \tag{32}$$

This system (32) has an unstable parasite-free equilibrium (0,0) and a unique parasite-positive equilibrium $E_1 = (I_h^*, I_v^*)$ if $\mathcal{R}_0 > 1$, where S_v^* is replaced by $S_v^0 - I_v^*$ for the susceptible vectors at equilibrium.

The Jacobian matrix at E_1 is

$$J(E_1) = \begin{pmatrix} -(\beta_h I_v^* + \mu_h) & \beta_h(N_h - I_h^*) \\ \beta_v(S_v^0 - I_v^*) & -\left(\frac{\beta_h\beta_v N_h S_v^0}{\beta_h I_v^* + \mu_h} + \beta_c I_v^*\right) \end{pmatrix},$$

and it has a negative trace, and a positive determinant

$$\det(J(E_1)) = \beta_h\beta_v S_v^0 I_h^* + \beta_c I_v^*(\beta_h I_v^* + \mu_h) + \beta_h\beta_v I_v^*(N_h - I_h^*).$$

Therefore, all eigenvalues of the matrix $J(E_1)$ have the negative real parts which implies E_1 is locally asymptotically stable.

We further denote

$$\begin{pmatrix} f_1(I_h, I_v) \\ f_2(I_h, I_v) \end{pmatrix} = \begin{pmatrix} \beta_h(N_h - I_h)I_v - \mu_h I_h \\ \beta_v I_h(S_v^0 - I_v) + \beta_c(S_v^0 - I_v)I_v - \mu_v I_v \end{pmatrix}.$$

Both f_1 and f_2: $\mathbb{R}_+^2 \to \mathbb{R}$ are continuously differentiable maps, and $\frac{\partial f_1}{\partial I_v} = \beta_h(N_h - I_h) \ge 0$ and $\frac{\partial f_2}{\partial I_h} = \beta_v(S_v^0 - I_v) \ge 0$, then system (32) is cooperative on a domain $D = \{(I_h, I_v) \in \mathbb{R}^2 : I_h \in [0, N_h], I_v \in [0, S_v^0]\}$. It is clear that, for $\mathcal{R}_0 > 1$, system (32) has a parasite-free equilibrium (0,0) which is unstable and a unique parasite-positive equilibrium E_1. Following Theorem 3.2.2 in [48], E_1 is global attractive. Subsequently, the parasite-positive equilibrium E^* of sub-system (30) is globally asymptotically stable. □

Numerical simulations are conducted to examine the globally asymptotic stability of the parasite-positive equilibrium. Fig. 7 shows the dynamics of the populations I_h, S_v, I_v with two different sets of initial conditions, and both sets of solutions converge to the same steady state, as expected.

3.5. Occurrence of oscillation with pathogenic effect

In preceding subsection, We have presented the globally asymptotic stability of the parasite-positive equilibrium for the special case without pathogenic effect on the triatomine bugs. For the case with pathogenic effect, only some sufficient conditions are found to ensure the local stability. In this subsection, we numerically reveal the occurrence of sustained oscillations for the full model (7). For the purpose of illustration, all parameter values used are purely illustrative, though some are elaborated from Table 1.

With a fixed θ, Fig. 8 shows the appearance of sustained oscillations by increasing the parasite-induced death rate of vectors d_v from 0.02025, to 0.05 and 0.2, where the blue solid curves and red dashed ones correspond to the scenarios without and with co-feeding transmission ($\beta_c = 0$ or 0.05), respectively. For the relatively small d_v in Fig. 8(a), the solutions of $I_h(t)$ tends to the positive equilibrium, exhibiting no oscillation. By increasing d_v in Fig. 8(b and c), we observe that sustained oscillations occur, and a larger amplitude is related to a larger d_v, moreover the presence of co-feeding transmission reduces the amplitude of oscillations.

With a fixed d_v, Fig. 9 shows the disappearance of sustained oscillation by increasing θ from 0.0005 to 0.005 and 0.01825, where the blue solid curves and red dashed ones correspond to the cases without and with co-feeding transmission ($\beta_c = 0$ or 0.005), respectively. Compared to Fig. 8, we observe disappearance rather than occurrence of the sustained oscillations with the increased θ, and a larger amplitude of oscillation is conversely related to a smaller θ. However, it is the same that the role of co-feeding transmission is to reduce the amplitude of oscillations as shown in Fig. 9(a and b).

In short, we find that a larger d_v or a smaller θ can lead to the easier occurrence of sustained oscillations for system (7), which indicates the loss of structural stability. While, the co-feeding transmission has a negative impact on the amplitude of oscillation, hence stabilizes the system. Biologically, this implies that apart from seasonal variation, we have shown another mechanism for the occurrence of sustained oscillations or the periodic cycles of triatomine bug population for Chagas disease transmission, where bugs' pathogenicity plays an important role.

4. Discussion and conclusion

In this work, we have developed a novel model which captures two routes of *T. rangeli* parasite transmission, normal insect-host-insect systemic transmission and insect-to-insect co-feeding transmission when both infected and susceptible bugs are co-feeding on the same hosts. In addition, pathogenic effect on triatomine bug population is also taken into account. Though *T. rangeli* is not pathogenic to human beings, it is pathogenic to triatomine bugs. This greatly affects the dynamics of *T. rangeli* parasite population and triatomine bug population, which is closely related to the risk of Chagas disease and the potential cost of vaccine development in domestic animals [50,51]. We have found the conditions for the persistence and extinction of *T. rangeli* parasite and its vector populations by analyzing the long-term dynamics of the model, which could provide some critical insights for the prevention and control of Chagas disease.

Theoretically, two thresholds $\mathcal{R}_v$ and $\mathcal{R}_0$ have been derived to characterize the dynamical behavior of the model, which is summarized in Table 2 for the convenience of readers. We have shown that triatomine bug population dies out if $\mathcal{R}_v < 1$, implying no risk of Chagas disease. If $\mathcal{R}_v > 1$, triatomine bug population changes to persist, indicating the potential risk to Chagas disease. We further found that infected host and vector populations will go extinct if $\mathcal{R}_0 < 1$, indicating no impact of *T. rangeli* parasite on host and triatomine bug populations at long-term dynamics, thus no risk of Chagas disease. If the condition of $\mathcal{R}_0 > 1$ is satisfied, host population with positive *T. rangeli* parasite will persist which could lead to the possible false positive diagnosis of Chagas disease [10]. Moreover, we numerically found in Figs. 5 and 6 that the total population size of triatomine bugs is increased with the decrease of competent hosts or the increase of quasi-competent hosts, which could result in an increase in the risk of getting Chagas disease.

Oscillation phenomenon is very common for vector-borne diseases. In general, delay differential equations, where delays naturally occur in vector-borne diseases, are frequently used to model the observed and/or unobserved oscillations [16,43]. For instance, by introducing a delay τ into the recruitment rate of new susceptible triatomine bugs, where τ is the time required for eggs to develop into sexually mature adults, Velasco-Hernández has successfully simulated the fluctuating behaviors of model solutions and compared to the field data [16]. By including a delayed logistic growth term and with interrupted spraying schedules,

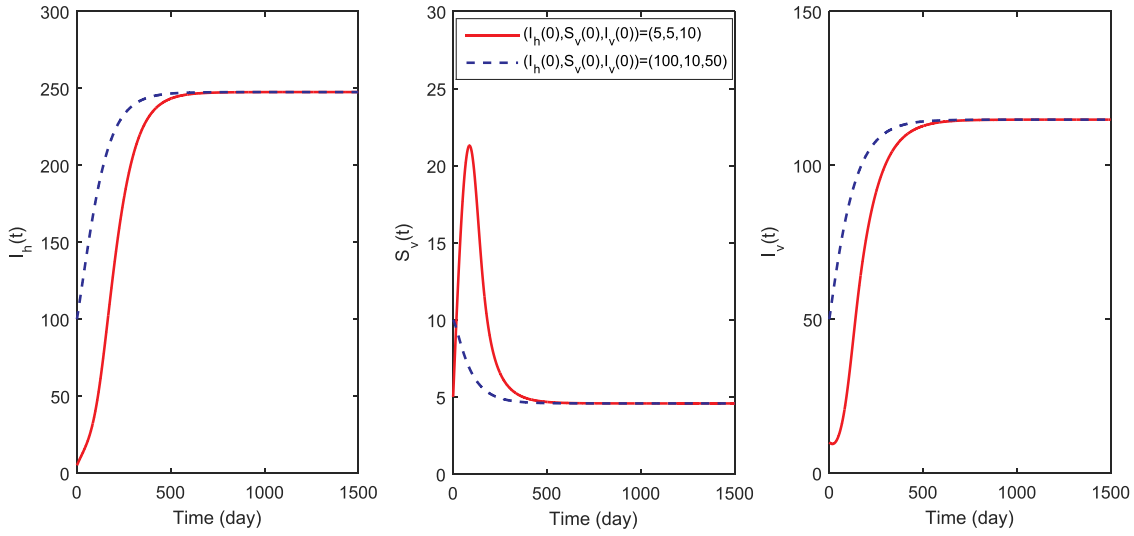

Fig. 7. Numerical solutions of model (7) without pathogenic effect on triatomine bugs. The parameter values are given $\theta = 1$, $d_v = 0$, $N_h = 300$, $N_q = 50$, $\alpha = 1$, $a = 0.6$, $b = 0.06$, $c = 0.49$, $\mu_h = 0.0025$, $\mu_v = 0.0083$, $r = 0.0274$, $\sigma = 0.01$, $\omega = 1$, $\tau_1 = \tau_2 = 15/60/24$, $\delta = 0.5$, $\beta_{ch} = 0.005$, $\beta_{cq} = 0.001$, where $\mathcal{R}_0 > 1$.

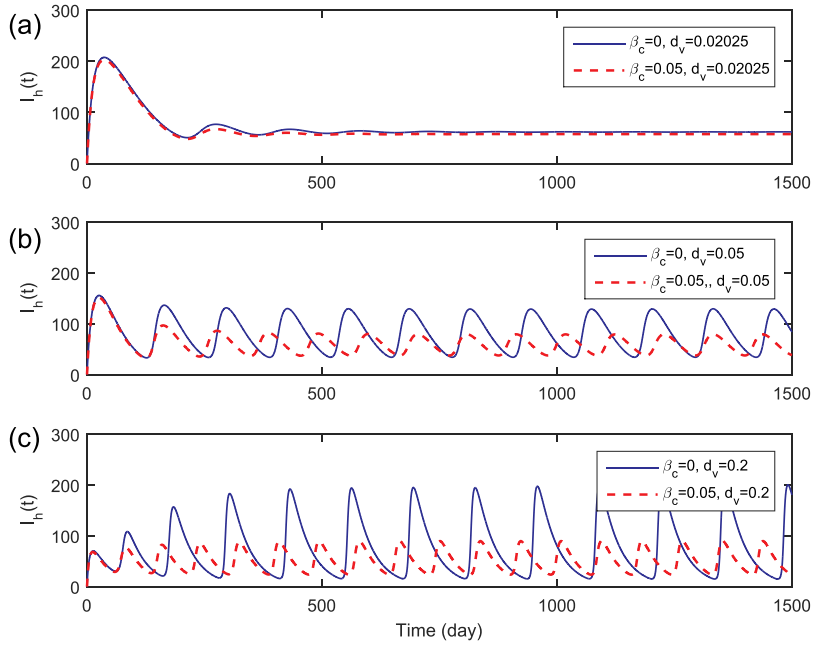

Fig. 8. Oscillation appearance of system (7) varying with d_v and β_c. (a) $d_v = 0.02025$, (b) $d_v = 0.05$, (c) $d_v = 0.2$, moreover, each plot considers $\beta_c = 0$ and 0.05. Other parameter values are $r = 0.5$, $\sigma = 0.0001$, $\mu_h = 0.025$, $\mu_v = 0.005$, $N_h = 400$, $\beta_h = 0.005$, $\beta_v = 0.01$, $\theta = 0.01$, here from top to bottom $\mathcal{R}_0 > 1$.

Spagnuolo and co-authors have studied the fluctuating outcomes for Chagas disease [52]. Other types of ordinary differential equations (ODEs), that include seasonality and/or cyclic control strategies such as insecticide spraying, have also been utilized to simulate the oscillations of the model solutions [53,54]. In the present study, we have developed a system of autonomous ODEs and observed the sustained oscillations in solutions, where the pathogenic effect of triatomine bugs plays a crucial role. More precisely, by adjusting the parameters d_v and θ, sustained oscillations are numerically observed; moreover, a larger d_v or a smaller θ leads to a larger amplitude of the oscillation. This finding is not only mathematically but also biologically important, because few ODE models with similar types of vector-borne disease transmissions can lead to solutions with fluctuating behaviors. It suggests that further biological investigation is necessary to identify the precise knowledge of the pathogenic effect on bugs.

A major limitation in this study is that the infection rates $\lambda_h(t)$, $\lambda_v(t)$ and $\lambda_c(t)$, which are based on the average idea, may be oversimplified. In particular, the contact rate a between hosts and vectors might be a piecewise function rather than a constant, since triatomine bugs attack sleeping or quiescent hosts during night. Moreover, the occurrence of the sustained oscillations and the corresponding amplitudes are only illustrated by numerical examples with the chosen typical parameters, and a thorough theoretical investigation is desirable to identify the critical conditions and understand the properties of sustained oscillations.

Despite the progress in understanding the complexity of host-parasite-vector interaction, our knowledge of the interaction of *T. rangeli* parasite and *R. prolixus* vectors remains far from complete. In future research, this model could be adapted to include the *T. cruzi* parasite to understand the impact of co-infection on the successful transmission of Chagas disease, since *T. cruzi* is the causative agent and it shares a diversity of common mammal hosts and triatomine species with *T. rangeli*.

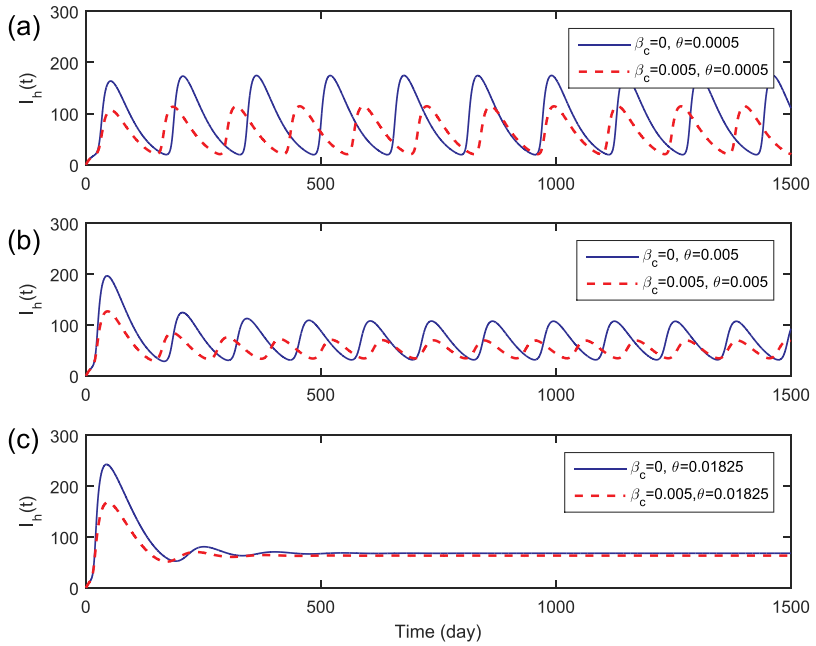

Fig. 9. Oscillation appearance of system (7) varying with θ. (a) $\theta = 0.0005$, (b) $\theta = 0.005$, (c) $\theta = 0.01825$, moreover, each plot considers $\beta_c = 0$ and 0.005. Other parameter values are $r = 0.5$, $\sigma = 0.001$, $\mu_h = 0.025$, $\mu_v = 0.05$, $N_h = 400$, $\beta_h = 0.0005$, $\beta_v = 0.01$, $d_v = 0.002$, here $\mathcal{R}_0 > 1$.

To the best of our knowledge, the *T. cruzi* transmission and its vector behavior are different from those of *T. rangeli*, namely, the former has no co-feeding transmission and no pathogenic effect on its vectors.

Declaration of Competing Interest

The authors declare that they do not have any financial or non-financial conflict of interests.

Acknowledgments

The authors would like to thank the financial support from the National Natural Science Foundation of China (11501358 by XW and 11601336 by DG), the Natural Sciences and Engineering Research Council of Canada and the Canada Research Chairs program (JW). D. Gao also thanks the support of the Program for Professor of Special Appointment (Eastern Scholar) at Shanghai Institutions of Higher Learning, and the Shanghai Gaofeng Project for the University Academic Development Program. The authors would like to thank two anonymous referees for their helpful and insightful comments.

Appendix A. Proof of Theorem 4.

Proof. For simplicity, we omit the subscript '*' for each variable at equilibrium. Let the right sides in system (7) be zeros, namely

$$\beta_h(N_h - I_h)I_v - \mu_h I_h = 0, \tag{A.1}$$

$$r(S_v + \theta I_v)e^{-\sigma(S_v+I_v)} - \beta_v I_h S_v - \beta_c S_v I_v - \mu_v S_v = 0, \tag{A.2}$$

$$\beta_v I_h S_v + \beta_c S_v I_v - (d_v + \mu_v)I_v = 0. \tag{A.3}$$

Solving Eq. (A.1) and Eq. (A.3), we have

$$I_h = \frac{\beta_h I_v}{\beta_h I_v + \mu_h} N_h, \quad S_v = \frac{g_1 I_v + \omega_1}{g_2 I_v + \omega_2}, \tag{A.4}$$

where

$$g_1 = \beta_h(d_v + \mu_v),\ g_2 = \beta_h\beta_c,\ \omega_1 = \mu_h(d_v + \mu_v),\ \omega_2 = \mu_h\beta_c + \beta_h\beta_v N_h. \tag{A.5}$$

Considering $I_v \neq 0$. Adding Eqs. (A.2) and (A.3) together and using the expression of S_v in terms of I_v, we obtain

$$r\left(\frac{g_1 I_v + \omega_1}{g_2 I_v + \omega_2} + \theta I_v\right)e^{-\sigma\left(\frac{g_1 I_v+\omega_1}{g_2 I_v+\omega_2}+I_v\right)} = d_v I_v + \mu_v\left(\frac{g_1 I_v + \omega_1}{g_2 I_v + \omega_2} + I_v\right), \tag{A.6}$$

which plays a critical role in determining the existence of positive solution of I_v. To do this, shifting the term $r\left(\frac{g_1 I_v + \omega_1}{g_2 I_v + \omega_2} + \theta I_v\right)$ to the right side yields

$$e^{-\sigma\left(\frac{g_1 I_v+\omega_1}{g_2 I_v+\omega_2}+I_v\right)} = \frac{d_v I_v + \mu_v\left(\frac{g_1 I_v + \omega_1}{g_2 I_v + \omega_2} + I_v\right)}{r\left(\frac{g_1 I_v + \omega_1}{g_2 I_v + \omega_2} + \theta I_v\right)}, \tag{A.7}$$

and denote functions F: $I_v \in \mathbb{R}_+ \to \mathbb{R}$ and G: $I_v \in \mathbb{R}_+ \to \mathbb{R}$ as

$$F(I_v) = e^{-\sigma\left(\frac{g_1 I_v+\omega_1}{g_2 I_v+\omega_2}+I_v\right)}, \quad G(I_v) = \frac{d_v I_v + \mu_v\left(\frac{g_1 I_v+\omega_1}{g_2 I_v+\omega_2}+I_v\right)}{r\left(\frac{g_1 I_v+\omega_1}{g_2 I_v+\omega_2}+\theta I_v\right)}. \tag{A.8}$$

We can determine the monotonicity of functions F and G with respect to I_v. Since we have

$$\frac{g_1}{g_2} = \frac{d_v+\mu_v}{\beta_c} > \frac{\omega_1}{\omega_2} = \frac{\mu_h(d_v+\mu_v)}{\mu_h\beta_c+\beta_h\beta_v N_h},$$

thus we have

$$F'(I_v) = -\sigma\cdot e^{-\sigma\left(\frac{g_1 I_v+\omega_1}{g_2 I_v+\omega_2}+I_v\right)}\cdot\left(\frac{g_1\omega_2-\omega_1 g_2}{(g_2 I_v+\omega_2)^2}+1\right) < 0.$$

Moreover, we have

$$G'(I_v) = \frac{(d_v+\mu_v(1-\theta))(g_1 g_2 I_v^2 + 2w_1 g_2 I_v + w_1 w_2)}{(\theta r g_2 I_v^2 + (r g_1 + \theta r w_2) I_v + r w_1)^2} > 0,$$

then we obtain that $F(I_v)$ is monotonically decreasing and $G(I_v)$ is monotonically increasing with respect to $I_v \geq 0$.

Moreover, we can find that

$$\max_{I_v\geq 0} F(I_v) = F(0) = e^{-\sigma\frac{\omega_1}{\omega_2}}, \quad \lim_{I_v\to+\infty} F(I_v) = 0,$$

and

$$\min_{I_v\geq 0} G(I_v) = G(0) = \frac{\mu_v}{r}, \quad \lim_{I_v\to+\infty} G(I_v) = \frac{d_v+\mu_v}{\theta r}.$$

Accordingly, Eq. (A.6) has a unique positive solution $I_v^* > 0$ if and only if $F(0) > G(0)$, that is,

$$e^{-\sigma\frac{d_v+\mu_v}{\beta_c+\beta_h\beta_v N_h/\mu_h}} > \frac{\mu_v}{r}. \tag{A.9}$$

Taking Logarithm on both sides in inequality (A.9) leads to

$$\frac{\beta_c S_v^0}{d_v+\mu_v} + \frac{\beta_h N_h \beta_v S_v^0}{\mu_h(d_v+\mu_v)} > 1 \iff \mathcal{R}_w + \mathcal{R}_{hv}^2 > 1.$$

Multiplying 4 and then adding the term $(\frac{\beta_c S_v^0}{d_v+\mu_v})^2$ at both sides on the above inequality, we can have

$$\left(\frac{\beta_c S_v^0}{d_v+\mu_v}\right)^2 + 4\frac{\beta_h N_h\beta_v S_v^0}{\mu_h(d_v+\mu_v)} > 4 - 4\frac{\beta_c S_v^0}{d_v+\mu_v} + \left(\frac{\beta_c S_v^0}{d_v+\mu_v}\right)^2 = \left(2-\frac{\beta_c S_v^0}{d_v+\mu_v}\right)^2. \tag{A.10}$$

Taking square root and a simple algebraic calculation, we obtain

$$\frac{1}{2}\left(\frac{\beta_c S_v^0}{d_v+\mu_v} + \sqrt{\left(\frac{\beta_c S_v^0}{d_v+\mu_v}\right)^2 + 4\frac{\beta_h\beta_v N_h S_v^0}{\mu_h(d_v+\mu_v)}}\right) > 1,$$

namely,

$\mathcal{R}_0 > 1$.

□

References

[1] J.A. Rassi, A. Rassi, J.A. Marin-Neto, Chagas disease, Lancet 375 (2010) 1388–1402, https://doi.org/10.1016/S0140-6736(10)60061-X.

[2] B. Pecoul, C. Batista, E. Stobbaerts, I. Ribeiro, R. Vilasanjuan, J. Gascon, M.J. Pinazo, S. Moriana, S. Gold, A. Pereiro, M. Navarro, F. Torrico, M.E. Bottazzi, P.J. Hotez, The BENEFIT trial: where do we go from here? PLoS Negl. Trop. Dis. 10 (2) (2016) e0004343, https://doi.org/10.1371/journal.pntd.0004343.

[3] B.Y. Lee, S.M. Bartsch, L. Skrip, D.L. Hertenstein, C.M. Avelis, M. Ndeffo-Mbah, C. Tilchin, E. Dumonteil, A. Galvani, Are the london declaration's 2020 goals sufficient to control chagas disease? Modeling scenarios for the Yucatan Peninsula, PLoS Negl. Trop. Dis. 12 (3) (2018) e0006337, https://doi.org/10.1371/journal.pntd.0006337.

[4] A.B.B. De Oliveira, K.C.C. Alevi, C.H.L. Imperador, F.F. Madeira, M.T.V. Azeredo-Oliveira, Parasite–vector interaction of chagas disease: a mini-review, Am. J. Trop. Med. Hyg. 98 (2018) 653–655, https://doi.org/10.4269/ajtmh.17-0657.

[5] A. Requena-Méndez, E. Aldasoro, E. de Lazzari, E. Sicuri, M. Brown, J. Gascon, J. Muñoz, Prevalence of chagas disease in latin-american migrants living in europe: a systematic review and meta-analysis, PLoS Negl. Trop. Dis. 9 (2015) e0003540, https://doi.org/10.1371/journal.pntd.0003540.

[6] J.P. Pierre, K. Kamran, N. Momar, Congenitally transmitted chagas disease in canada: a family cluster, CMAJ 189 (2017) E1489–E1492, https://doi.org/10.1503/cmaj.170648.

[7] C. Bern, Chagas' disease, N. Engl. J. Med. 373 (2015) 456–466, https://doi.org/10.1056/NEJMra1410150.

[8] N. Tomasini, P.G. Ragone, S. Gourbiére, J.P. Aparicio, P. Diosque, Epidemiological modeling of *trypanosoma cruzi*: low stercorarian transmission and failure of host adaptive immunity explain the frequency of mixed infections in humans, PLoS Comput. Biol. 13 (5) (2017) e1005532, https://doi.org/10.1371/journal.pcbi.1005532.

[9] Triatomine bugs-world health organization, https://www.who.int/water_sanitation_health/resources/vector210to222.pdf. Accessed on 2019/08/06.

[10] R.C. Ferreira, C.F. Teixeira, V.F.A. de Sousa, A.A. Guarneri, Effect of temperature and vector nutrition on the development and multiplication of *trypanosoma rangeli* in *rhodnius prolixus*, Parasitol. Res. 117 (6) (2018) 1737–1744, https://doi.org/10.1007/s00436-018-5854-2.

[11] S. Schorderet-Weber, S. Noack, P.M. Selzer, R. Kaminsky, Blocking transmission of

vector-borne diseases, Int. J. Parasitol. Drugs Drug Resist. 7 (1) (2017) 90–109, https://doi.org/10.1016/j.ijpddr.2017.01.004.
[12] M.A. Acuña Zegarra, D. Olmos-Liceaga, J.X. Velasco-Hernández, The role of animal grazing in the spread of chagas disease, J. Theor. Biol. 457 (2018) 19–28, https://doi.org/10.1016/j.jtbi.2018.08.025.
[13] C. Bern, S. Kjos, M.J. Yabsley, S.P. Montgomery, *Trypanosoma cruzi* and chagas' disease in the united states, Clin. Microbiol. Rev. 24 (4) (2011) 655–681, https://doi.org/10.1128/CMR.00005-11.
[14] R.E. Gürtler, M.V. Cardinal, Reservoir host competence and the role of domestic and commensal hosts in the transmission of *trypanosoma cruzi*, Acta Trop. 151 (2015) 32–50, https://doi.org/10.1016/j.actatropica.2015.05.029.
[15] J.X. Velasco-Hernández, An epidemiological model for the dynamics of chagas disease, BioSystems 26 (2) (1991) 127–134, https://doi.org/10.1016/0303-2647(91)90043-k.
[16] J.X. Velasco-Hernández, A model for chagas disease involving transmission by vectors and blood transfusion, Theor. Popul. Biol. 46 (1) (1994) 1–31, https://doi.org/10.1006/tpbi.1994.1017.
[17] L. Stevens, D.M. Rizzo, D.E. Lucero, J.C. Pizarro, Household model of chagas disease vectors (hemiptera: Reduviidae) considering domestic, peridomestic, and sylvatic vector populations, J. Med. Entomol. 50 (4) (2013) 907–915, https://doi.org/10.1603/me12096.
[18] C.J. Schofield, N.G. Williams, T.F. Marshall, Density-dependent perception of triatomine bug bites, Ann. Trop. Med. Parasitol. 80 (3) (1986) 351–358, https://doi.org/10.1080/00034983.1986.11812028.
[19] R. Gurgel-GonÃ§ alves, C. Galvao, J. Costa, A.T. Peterson, Geographic distribution of chagas disease vectors in brazil based on ecological niche modeling, J. Trop. Med. 2012 (2012) 705326, https://doi.org/10.1155/2012/705326.
[20] F. Lardeux, Niche invasion, competition and coexistence amongst wild and domestic bolivian populations of chagas vector *triatoma infestans* (hemiptera, reduviidae, triatominae), C. R. Biol. 336 (4) (2013) 183–193, https://doi.org/10.1016/j.crvi.2013.05.003.
[21] C. Barbu, E. Dumonteil, S. Gourbiére, Characterization of the dispersal of non-domiciliated triatoma dimidiata through the selection of spatially explicit models, PLoS Negl. Trop. Dis. 4 (8) (2010) e777, https://doi.org/10.1371/journal.pntd.0000-777.
[22] C.M. Barbu, A. Hong, J.M. Manne, D.S. Small, J.E. Quintanilla Calderón, K. Sethuraman, V. Quispe-Machaca, J. Ancca-Juárez, J.G. Cornejo del Carpio, F.S. MÃ!'laga Chavez, C. Náquira, M.Z. Levy, The effects of city streets on an urban disease vector, PLoS Comput. Biol. 9 (1) (2013) e1002801, https://doi.org/10.1371/journal.pcbi.1002801.
[23] H. Inaba, H. Sekine, A mathematical model for chagas disease with infection-age dependent infectivity, Math. Biosci. 190 (1) (2004) 39–69, https://doi.org/10.1016/j.mbs.2004.02.004.
[24] C.M. Kribs, C. Mitchell, Host switching vs. host sharing in overlapping sylvatic *trypanosoma cruzi* transmission cycles, J. Biol. Dyn. 9 (1) (2015) 247–277, https://doi.org/10.1080/17513758.2015.1075611.
[25] J.K. Peterson, S.M. Bartsch, B.Y. Lee, A.P. Dobson, Broad patterns in domestic vector-borne *trypanosoma cruzi* transmission dynamics: synanthropic animals and vector control, Parasit. Vectors 8 (2015) 537, https://doi.org/10.1186/s13071-015-1146-1.
[26] R.E. Gürtler, L.A. Ceballos, P. Ordóñez Krasnowski, L.A. Lanati, R. Stariolo, U. Kitron, Strong host-feeding preferences of the vector triatoma infestans modified by vector density: implications for the epidemiology of chagas disease, PLoS Negl. Trop. Dis. 3 (5) (2009) e447, https://doi.org/10.1371/journal.pntd.0000447.
[27] C. Barbu, E. Dumonteil, S. Gourbiére, Optimization of control strategies for non-domiciliated *triatoma dimidiata*, chagas disease vector in the yucatan peninsula, mexico, PLoS Negl. Trop. Dis. 3 (4) (2009) e416, https://doi.org/10.1371/journal.pntd.0000416.
[28] M.Z. Levy, F.S. Malaga Chavez, J.G. Cornejo Del Carpio, D.A. Vilhena, F.E. McKenzie, J.B. Plotkin, Rational spatio-temporal strategies for controlling a chagas disease vector in urban environments, J. R. Soc. Interface 7 (48) (2010) 1061–1070, https://doi.org/10.1098/rsif.2009.0479.
[29] R.E. Gürtler, U. Kitron, M.C. Cecere, E.L. Segura, J.E. Cohen, Sustainable vector control and management of chagas disease in the Gran Vhaco, argentina, Proc. Natl. Acad. Sci. USA 104 (41) (2007) 16194–16199, https://doi.org/10.1073/pnas.0700863104.
[30] B.Y. Lee, K.M. Bacon, A.R. Wateska, M.E. Bottazzi, E. Dumonteil, P.J. Hotez, Modeling the economic value of a chagas' disease therapeutic vaccine, Hum Vaccin Immunother 8 (9) (2012) 1293–1301. 10.4161/hv.20966
[31] B.Y. Lee, K.M. Bacon, M.E. Bottazzi, P.J. Hotez, Global economic burden of chagas disease: a computational simulation model, Lancet Infect. Dis. 13 (4) (2013) 342–348, https://doi.org/10.1016/S1473-3099(13)70002-1.
[32] A.A. Guarneri, M.G. Lorenzo, Triatomine physiology in the context of trypanosome infection, J. Insect. Physiol. 97 (2017) 66–76, https://doi.org/10.1016/j.jinsphys.2016.07.005.
[33] M.A. Miles, J.R. Arias, S.A. Valente, R.D. Naiff, A.A. de Souza, M.M. Povoa, J.A. Lima, R.A. Cedillos, Vertebrate hosts and vectors of *trypanosoma rangeli* in the amazon basin of brazil, Am. J. Trop. Med. Hyg. 32 (1983) 1251–1259, https://doi.org/10.4269/ajtmh.1983.32.1251.
[34] F. Maia da Silva, A.C. Rodrigues, M. Campaner, C.S.A. Takata, M.C. Brigido, A.C. Junqueira, J.R. Coura, G.F. Takeda, J.J. Shaw, M.M.G. Teixeira, Randomly amplified polymorphic DNA analysis of *trypanosoma rangeli* and allied species from human, monkeys and other sylvatic mammals of the brazilian amazon disclosed a new group and a speciesspecific marker, Parasitology 128 (2004) 283–294, https://doi.org/10.1017/S0031182003004554.
[35] J.K. Peterson, A.L. Graham, What is the 'true' effect of trypanosoma rangeli on its triatomine bug vector? J. Vector Ecol. 41 (1) (2016) 27–33, https://doi.org/10.1111/jvec. 12190.
[36] L. Ferreira Lde, M.H. Pereira, A.A. Guarneri, Revisiting *trypanosoma rangeli* transmission involving susceptible and non-susceptible hosts, PLoS One 10 (10) (2015) e0140575, https://doi.org/10.1371/journal.pone.0140575.
[37] W.G. Friend, J.J. Smith, Feeding in *rhodnius prolixus*: mouthpart activity and salivation, and their correlation with chinese of electrical resistance, J. Insect Physiol. 17 (2) (1971) 233–243, https://doi.org/10.1016/0022-1910(71)90207-1.
[38] A.C. Soares, J. Carvalho-Tavares, F. Gontijo Nde, V.C. dos Santos, M.M. Teixeira, M.H. Pereira, Salivation pattern of *rhodnius prolixus*(reduviidae; triatominae) in mouse skin, J. Insect Physiol. 52 (5) (2006) 468–472, https://doi.org/10.1016/j.jinsphys.2006.01.003.
[39] J.C. Nevoa, M.T. Mendes, M.V. da Silva, S.C. Soares, C.J.F. Oliveira, J.M.C. Ribeiro, An insight into the salivary gland and fat body transcriptome of *panstrongylus lignarius* (hemiptera: heteroptera), The Main Vector of Chagas Disease in Peru 12 (2) (2018) e0006243, https://doi.org/10.1371/journal.pntd.0006243.
[40] S.E. Randolph, L. Gern, P.A. Nuttall, Co-feeding ticks: epidemiological significance for tick-borne pathogen transmission, Parasitol. Today 12 (12) (1996) 472–479, https://doi.org/10.1016/s0169-4758(96)10072-7.
[41] M.J. Voordouw, Co-feeding transmission in lyme disease pathogens, Parasitology 142 (2) (2014) 290–302, https://doi.org/10.1017/S0031182014001486.
[42] K. Nah, F.M.G. Magpantay, A. Bede-Fazekas, G. Röst, A.J. Trájer, X. Wu, X. Zhang, J. Wu, Assessing systemic and non-systemic transmission risk of tick-borne encephalitis virus in hungary, PLoS One 14 (6) (2019) e0217206, https://doi.org/10.1371/journal.pone.0217206.
[43] X. Zhang, X. Wu, J. Wu, Critical contact rate for vector–host–pathogen oscillation involving co-feeding and diapause, J. Biol. Syst. 25 (4) (2017) 657–675, https://doi.org/10.1142/S0218339017400083.
[44] W.E. Ricker, Computation and Interpretation of Biological Statistics of Fish Populations, Bull. Fish. Res. Board Can. No. 191, Blackburn Press, Ottawa, 1975.
[45] J.E. Rabinovich, J.A. Leal, D. Feliciangeli de Piñero, Domiciliary biting frequency and blood ingestion of the chagas's disease vector *rhodnius prolixus stahl* (hemiptera: reduviidae in Venezuela), Trans. R. Soc. Trop. Med. Hyg. 73 (3) (1979) 272–283, https://doi.org/10.1016/0035-9203(79)90082-8.
[46] Z.M. Cucunuba, P. Nouvellet, J.K. Peterson, S.M. Bartsch, B.Y. Lee, A.P. Dobson, M.G. Basanez, Complementary paths to chagas disease elimination: the impact of combining vector control with etiological treatment, Clin. Infect Dis. 66 (suppl4) (2018) S293–S300, https://doi.org/10.1093/cid/ciy006.
[47] N. Añez, E. Nieves, D. Cazorla, Studies on *trypanosoma rangeli* tejera, 1920. IX. Course of infection in different stages of *rhodnius prolixus*, Mem. Inst. Oswaldo Cruz 82 (1987) 1–6, https://doi.org/10.1590/s0074-02761987000100001.
[48] H.L. Smith, Monotone dynamical systems: an introduction to the theory of competitive and cooperative systems, Am. Math. Soc. Math. Surv. Monogr. (1995).
[49] P. van den Driessche, J. Watmough, Reproduction numbers and sub-threshold endemic equilibria for compartmental models of disease transmission, Math Biosci. 180 (2002) 29–48, https://doi.org/10.1016/S0025-5564(02)00108-6.
[50] B. Basso, I. Castro, V. Introini, P. Gil, C. Truyens, E. Moretti, Vaccination with *trypanosoma rangeli* reduced the infectiousness of dogs experimentally infected with *trypanosome cruzi*, Vaccine. 25 (2007) 3855–3858, https://doi.org/10.1016/j.vaccine.2007.01.114.
[51] B. Basso, E. Moretti, R. Fretes, Vaccination with *trypanosoma rangeli* induces resistance of guinea pigs to virulent *trypanosome cruzi*, Vet. Immunol. Immunopathol. 157 (2014) 119–123, https://doi.org/10.1016/j.vetimm.2013.10.011.
[52] A.M. Spagnuolo, M. Shillor, L. Kingsland, A. Thatcher, M. Toeniskoetter, B. Wood, A logistic delay differential equation model for chagas disease with interrupted spraying schedules, J. Biol. Dyn. 6 (2012) 377–394, https://doi.org/10.1080/17513758.2011.587896.
[53] J.r. Coffield D. J., A.M. Spagnuolo, M. Shillor, E. Mema, B. Pell, A. Pruzinsky, A. Zetye, A model for chagas disease with oral and congenital transmission, PLoS One 8 (6) (2013) e67267, https://doi.org/10.1371/journal.pone.0067267.
[54] X. Wu, G. Röst, X. Zou, Impact of spring bird migration on the range expansion of ixodes Scapularis tick population, Bull. Math. Biol. 78 (1) (2016) 138–168, https://doi.org/10.1007/s11538-015-0133-1.